Journal of Environmental Sciences 160 (2026) 424–438

Contents lists available at ScienceDirect

Journal of Environmental Sciences

journal homepage: www.elsevier.com/locate/jes

JES JOURNAL OF ENVIRONMENTAL SCIENCES www.jesc.ac.cn

Research Article

Effectiveness of conventional municipal wastewater treatment plants in microplastics removal: Insights from multiple analytical techniques

Simone Cavazzoli[a,*], Costanza Scopetani[b], David Chelazzi[b], Tania Martellini[b], Alessandra Cincinelli[b], Emiliano Carretti[b], Miriam Ascolese[c], Riccardo Gori[d], Karl Mair[e], Werner Tirler[f], Massimo Donegà[f], Gianni Andreottola[a]

[a] Department of Civil, Environmental and Mechanical Engineering (DICAM), University of Trento, via Mesiano, 77 38123 Trento TN, Italy
[b] Chemistry Department 'Ugo Schiff' (DICUS) and Center for Colloid and Surface Science (CSGI), University of Florence, Via della Lastruccia, 13 50019 Sesto Fiorentino FI, Italy
[c] Department of Experimental and Clinical Medicine (DMSC), University of Florence, Largo Brambilla, 3 50134 Firenze FI, Italy
[d] Department of Civil and Environmental Engineering (DICEA), University of Florence, Via di Santa Marta, 3 50139 Firenze FI, Italy
[e] Eco Center S.p.a., Lungo Isarco Destro, 21° 39100 Bolzano BZ, Italy
[f] Eco Research, Via Luigi Negrelli, 13 39100 Bolzano BZ, Italy

ARTICLE INFO

Keywords:
Emerging contaminant
Plastic pollution
Analytical method
Spectroscopy
Spectrometry
MPs in WWTPs

ABSTRACT

This study investigated microplastics (MPs) sized 10–5000 μm across stages of a conventional municipal wastewater treatment plant using multiple analytical techniques. Samples were collected via pumping and filtration, treated with the Fenton reaction for wet peroxidation, and separated by density separation. Analysis employed Focal Plane Array Micro-Fourier Transform Infrared Spectroscopy (FPA micro-FTIR), a widely used technique in MPs analysis, alongside the less common Laser Direct Infrared Spectroscopy (LDIR), providing complementary data on particle composition, shape, size, and colour. To enhance insights, spectroscopic methods were supplemented with Thermal Desorption Gas Chromatography-Mass Spectrometry (TD-GC/MS), calibrated for specific polymers, to quantify MPs by mass and assess removal efficiency. Wastewater treatment effectively reduced MPs. In influent samples, concentrations reached 72 MPs/L (FTIR), 2117 MPs/L (LDIR), and 177 μg/L (TD-GC/MS). Primary treatments removed 41 %–55 %, while the wastewater treatment plant effluent contained 1 MPs/L (FTIR), 93 MPs/L (LDIR), and 2 μg/L (TD-GC/MS), reflecting 96 %–99 % removal efficiency. Activated sludge showed concentrations of 123 MPs/L (FTIR), 10,800 MPs/L (LDIR), and 0.3 mg/g dry weight (TD-GC/MS), underscoring its role in MPs capture. However, sludge dewatering released significant MPs into centrifuge rejected water: 484 MPs/L (FTIR), 23,000 MPs/L (LDIR), and 1100 μg/L (TD-GC/MS). These results highlight the effectiveness of conventional treatments in MPs removal and the critical role of sludge in capturing these contaminants. However, sludge dewatering poses a risk of reintroducing MPs into the environment. Effective sludge management should prioritize nutrient recovery and biomass valorisation to mitigate these risks and minimise harmful environmental impacts.

1. Introduction

Plastic production has grown significantly worldwide in recent decades, causing a major impact in terms of environmental contamination by plastic waste (Geyer et al., 2017). The durability, light weight and resistance to degradation of plastics have led to their wide use in various industries but also increase the likelihood of their release into the environment. The most prevalent polymers are obtained from fossil fuels and are the most widespread in the environment as contaminants. Polypropylene (PP), polyethylene (PE), polyvinyl chloride (PVC), polyethylene terephthalate (PET), polyurethane (PU), and polystyrene (PS) are the most globally produced polymers (Palacios-Mateo et al., 2021; Plastics Europe, 2024). Other polymers are widely used worldwide. For example, polybutadiene rubber (PBR), made from the polymerization of 1,3-butadiene, is known for its high wear resistance and is primarily used in tire manufacturing, accounting for 70 % of its production. It also enhances toughness in plastics like PS and acrylonitrile butadiene styrene (ABS) and is used in electronics due to its electrical resistivity. About 1 kg of PBR is used per car tire and 3.3 kg in utility vehicles (Brandt et al., 2011). Ethylene vinyl acetate (EVA) is a versatile, cost-effective material prized for its shock-absorbing properties, commonly used in footwear, plastic wraps, sports padding, and

* Corresponding author.
E-mail address: simone.cavazzoli@unitn.it (S. Cavazzoli).

https://doi.org/10.1016/j.jes.2025.04.035
Received 22 October 2024; Received in revised form 10 April 2025; Accepted 12 April 2025
Available online 15 April 2025

adhesives. It also finds applications in high-quality paints and biomedical devices like drug-delivery systems (Ogawa et al., 2012). Polyacrylonitrile (PAN), produced from acrylonitrile polymerization, is mainly used for synthetic fibers known for their durability and strength, and as a precursor for carbon fiber production. Acrylate polymers are valued for their transparency, break resistance, and elasticity. They are used in cosmetics, adhesives, automotive applications, and paints. Sodium polyacrylate, a superabsorbent polymer, is essential in disposable diapers (Penzel, 2000). Polymethylmethacrylate (PMMA), or acrylic glass, is a clear, break-resistant material, also used as rheology modifiers in cosmetics, while polyacrylamide copolymers aid in water treatment (Stickler and Rhein, 2000). Microplastics (MPs), i.e., small plastic particles with dimensions ranging from 5 mm to 1 μm, recently emerged as a pressing environmental issue, raising concerns due to their widespread presence in many ecosystems, including natural parks and protected or remote areas (Giarrizzo et al., 2019; Queiroz et al., 2022; Scopetani et al., 2021). Addressing the challenges posed by MPs pollution requires a comprehensive understanding of their sources, fate, and potential impact on the environment and human health. MPs can come from both primary and secondary sources, where larger plastic objects break down into smaller particles over time (Thompson et al., 2004). These MPs can act as carriers for harmful substances, such as organic and inorganic contaminants, as well as pathogens and antibiotic resistance genes (Bakir et al., 2012; Galafassi et al., 2021; Li et al., 2018; Rochman et al., 2013). Organisms exposed to MPs may experience ecotoxicity, and given their resistance to degradation, MPs may bioaccumulate up the trophic chain (Paul et al., 2020).

Wastewater treatment plants (WWTPs) collect MPs from municipal and industrial wastewater (Blair et al., 2017). Upstream sources of MPs include synthetic fibres from clothing washes, primary MPs contained in personal hygiene products, and road particles from areas without separate sewerage systems (European Commission, 2023). Several studies have shown that WWTPs can remove up to 98 % of MPs, with higher removal rates in plants using tertiary treatments like sand/disk filters or membrane technologies (Ben-David et al., 2021; Simon et al., 2018; Talvitie et al., 2017a). Understanding the role of WWTPs in capturing and removing MPs is crucial, as is identifying the most effective technologies to minimize their environmental release. During primary treatments, which include screening, grit and grease removal, 35 % to 59 % of MPs are removed (Rout et al., 2022). Larger particles are removed through screening and grit chambers, while aeration generates bubbles that lift MPs to the surface for skimming. Primary treatment achieves 50 % to 98 % MPs removal through surface skimming, gravity separation, and adsorption (Rout et al., 2022). Pretreatments and primary sedimentation are more effective at removing fibers than fragments, as fibers get trapped in flocculating particles and are separated during sedimentation. After biological treatment and final clarification, MPs in treated wastewater are reduced to 0.2 %-14 % of their initial concentration. MPs accumulate in sludge flocs and bacterial extracellular polymers in the aeration tank, eventually settling in the secondary clarification tank (Ali et al., 2021). Longer MPs/wastewater contact times during treatment can promote biofilm formation on MPs, altering their properties and enhancing their removal (Debroy et al., 2022). Although tertiary treatments (e.g., membrane bioreactor, sand filtration, and disc filters) further reduce MPs content in treated wastewaters, smaller MPs (< 200 μm) become more abundant downstream of tertiary treatment (Sun et al., 2019). Sewage sludge contains MPs concentrations ranging from 400 to 7000 particles/kg wt (wet weight) or approximately 1500–170,000 particles/kg dw (dry weight) (Ali et al., 2021). MPs in sludge are typically larger than those in wastewater, with fibers comprising up to 80 %. Synthetic fibers serve as reliable indicators of contamination in areas where sludge is applied to land, soil, and surface waters. Skimming units demonstrate the highest transfer of MPs to sludge, underscoring the effectiveness of early-stage skimming in MP removal, which could be further enhanced by Salsness-like technology (Stroski, 2019). Anaerobically digested sludge typically contains five times more MPs than activated or membrane bioreactor sludge. Additionally, about 20 % of MPs in sewage sludge re-enter the wastewater stream through sludge dewatering processes such as centrifugation (Salmi et al., 2021). Improperly managed sludge can release substantial quantities of MPs, along with associated pollutants and pathogens, into agricultural soils (Nizzetto et al., 2016). Co-pyrolysis with biomass provides a promising solution for treating MPs-contaminated sludge, enabling fuel production and chemical recovery while reducing environmental risks (Anuar Sharuddin et al., 2016).

Analysing MPs in WWTPs poses unique challenges, particularly with smaller fractions and nanoplastics (Cavazzoli et al., 2023). These tiny particles require specific analytical techniques for accurate detection and quantification. Quality assurance and control are critical for obtaining reliable data and evaluating potential environmental and human health impacts (Ziajahromi and Leusch, 2022). Moreover, the analytical method must be time-efficient to be practical for laboratories addressing micropollutants in wastewater. Adopting a multi-analytical approach, widely recommended in the literature, is crucial for accurately characterizing MPs in samples. However, this approach is rarely implemented, and the results from different analytical techniques are often difficult to compare (Adhikari et al., 2022). Focal Plane Array micro-FTIR (FPA micro-FTIR) is a non-destructive technique widely used in the analysis of MPs in environmental matrixes (Song et al., 2015). These instruments offer high-resolution in terms of MPs size enabling the analysis of MPs with dimensions down to 5-10 μm. However, FPA micro-FTIR-based instruments, if not automated, are time-consuming and require continuous manual handling of samples and data processing, which slows the process and makes it prone to human errors, potentially leading to inconsistencies in results (Primpke et al., 2018). The Laser Direct Infrared (LDIR) spectroscopic system is a relatively new tool in the field of MPs analysis in environmental samples. Consequently, validated preparation and measurement methods specific for LDIR aimed to ensure reproducible and valuable analyses are under development (Pagliaccia et al., 2025). Automated LDIR systems can analyse and map large amounts of data, allowing rapid and non-destructive screening of a high number of particles (Jia et al., 2022). Being an automated tool, it significantly reduces the need for manual sample manipulation and data processing, minimising the risk of human errors, and ensuring consistency and reproducibility in results (Dong et al., 2022). Consequently, automated systems like LDIR optimise the analytical process, reducing timeframes and maximising comparability between studies. An alternative to spectroscopic techniques for MPs analysis is thermal desorption gas chromatography coupled with mass spectrometry (TD-GC/MS), which operates at lower temperatures than pyrolytic GC/MS (Py-GC/MS), thereby preventing pyrolyzed product interference (Duemichen et al., 2019). TD-GC/MS can analyse larger sample volumes, in contrast to Py-GC/MS, which typically handle only 5 to 10 mg of material (Claessens et al., 2013). TD-GC/MS provides high sensitivity for detecting MPs at trace levels and can identify additives and chemical constituents (Endo et al., 2005). While TD-GC/MS efficiently process large sample volumes *via* automated systems, calibration with standard materials remains crucial due to the variability in polymer composition (Primpke et al., 2020). Studies that have analysed MPs with GC-MS techniques focused on a few polymers, such as PS, PE, and PP, while little has been done on the quantification of other polymers that are found in wastewater. Despite being a destructive technique, TD-GC/MS offers unique advantages. It enables the carrier flux exiting the desorber, containing thermodestruction products, to be split between the GC and an activated carbon vial. The vial adsorbs the released molecules, allowing for subsequent analysis using the GC/MS.

This research aims to identify, characterise, and quantify MPs in samples collected from various treatment stages of a municipal WWTP. A multi-analytical approach, incorporating FPA micro-FTIR, LDIR, and TD-GC/MS, will be employed to analyze MPs based on their number, mass, size, shape, and colour. The findings will be used to evaluate MPs dynamics, removal efficiency, and distribution throughout the wastew-

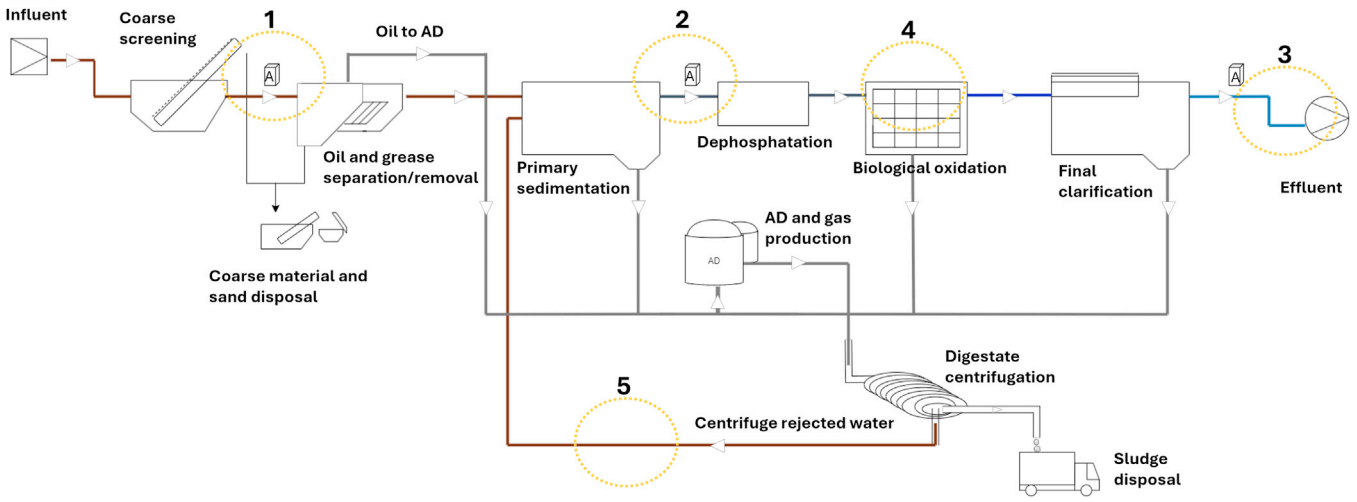

Fig. 1 – Diagram of the investigated wastewater treatment plant (WWTP). Sampling points 1-5 are highlighted with a dashed orange circle. A=autosamplers along the water purification line. Sampling points are highlighted with an orange dashed circle: (1) influent wastewater; (2) effluent from the primary clarifier; (3) WWTP effluent; (4) activated sludge sampled from the biological oxidation tank; (5) water extracted from the centrifuge, recirculated into the WWTP. Samples collected at points 1 and 2 collected using an autosampler (A, 24 h composite samples) and filtered using a pumping and filtration system (**Appendix A Fig. S1**). The sample at point 3 was accumulated over 24 h in a stainless-steel tank and subsequently filtered using the same pumping and filtration system. Samples from points 4 and 5 were collected as grab samples, as they were considered temporally homogeneous. AD: anaerobic digestion.

ater treatment process, as well as the environmental emission factors associated with the WWTP. A comparative analysis of the results from different analytical techniques will highlight their respective challenges and advantages, providing valuable insights for future studies.

2. Materials and methods

2.1. Description of the wastewater treatment plant

The study was conducted in the Alpine area of north-eastern Italy. Although the investigated WWTP is designed to serve a population equivalent (pe) of 450,000, it currently serves about 337,000 pe. In 2021 the plant processed approximately 42,294 m^3 of wastewater per day from 14 municipalities. The pretreatment process involves an initial screening step to remove coarse materials, such as wood, rags, and paper followed by grease and oil removal. Coarse materials and sand, after washing, are disposed of in a landfill, while collected oil and grease are routed to anaerobic digestion (AD) for biogas production. In the primary clarifier, finer particles settle and are subsequently scraped from the bottom of the tank and transferred to AD. The water leaving the primary clarifier flows into the biological oxidation tank, where microorganisms facilitate the transformation of biodegradable organic matter (OM) into biological sludge, as well as OM hydrolysis and mineralization. In the final clarifier, the biological sludge is separated from the water and directed to AD. A portion of the purified water is recycled within the plant as industrial water (~880,000 m^3). Once anaerobically digested, the sludge undergoes dewatering by centrifuge, before being transported to a designated disposal center. The centrifuge rejected water is reintroduced into the wastewater treatment line before the primary sedimentation. The methane generated during the AD of sewage sludge is utilized for electricity and heat generation, primarily to satisfy the energy needs of the WWTP.

2.2. Sampling points

For this study, samples were collected from the following points of the WWTP: (1) influent; (2) primary clarifier effluent; (3) WWTP effluent; (4) biological oxidation tank; (5) centrifuge rejected water. Fig. 1 provides a schematic representation of the WWTP under investigation, highlighting the selected sampling points. The chosen points along the treatment line allow for assessing the extent of MPs contamination in the influent (sampling point 1) and the efficiency of the WWTP in removing MPs during initial treatment stages (e.g., screening, grit and grease removal, primary sedimentation, (sampling point 2)) as well as across the entire treatment process (sampling point 3). Sampling points 4 and 5 (i.e., activated sludge and centrifuge rejected water) provide insights into what remains within the plant and is recirculated. Specifically, sludge flocs and bacterial extracellular metabolites in the aeration tank are known to accumulate MPs, while sludge dewatering processes prior to disposal may separate MPs along with the aqueous phase of the sludge (Fig. 1).

2.3. MPs sampling system

The influent (1) and the effluent of the primary clarifier (2) were sampled using an autosampler (MAXX SP5, MAXX Mess- und Probenahmetechnik GmbH, Germany), equipped with 10 L glass bottles (**Appendix A Fig. S1**). 3 L of (1) and 6 L of (2) were collected in a 24 h flow-weighted composite sample. This volume was then processed using an in-house made pump and filtration sampling system, consisting of a fully stainless-steel centrifugal pump (ENOS 20, Enoitalia S.r.l., Italy, 270 V, 50 Hz, q_{max}=30 L/min) connected to a 10 µm stainless-steel cartridge filter (MS stainless-steel screen cartridge, 4 7/8″ (124 mm), 10 µm, Wolftechnik Filtersysteme GmbH & Co. KG, Germany, PTFE gasket, PP filter housing). The sampling system is shown in **Appendix A Fig. S1**. The cartridge filters facilitated the concentration of suspended particulate matter, including MPs, on the filter surface and in approximately 200 mL of the filter housing liquid. A 1.5-bar overpressure valve was installed on the sampling system to maintain its integrity and prevent failures during sampling. After filtration, the cartridge filters and the filter housing liquid were transferred to a 1 L glass beaker with a metal lid and transported to the laboratory for MPs extraction.

The sampling time of the WWTP effluent (3) was adjusted according to the average hydraulic residence times of the wastewater within the WWTP. Specifically, the sampling of (3) was started with a 34-h delay relative to the influent sampling, as reported in **Appendix A Table S1**. This approach aimed to ensure that effluent samples were as consistent and representative as possible. Following the same rationale, the sampling of (2) began 1.5 h after the influent sampling. The final WWTP effluent was initially accumulated in a 500 L stainless-steel tank

pre-rinsed with ultrapure (UP) water, using a peristaltic pump (IPI96 (variant IPI96IN), Espango (Teknofluor S.r.l.), Italy, 230 V, 15-70 Hz) operating at a flow rate of 250 mL/min (**Appendix A Fig. S1**). Over 24 h, a total of 360 L was sampled. The effluent was then filtered using the previously described sampling system, employing a centrifugal pump to collect solids on a 10 μm stainless-steel cartridge filter. However, the filter became clogged before processing the full volume, causing the pump to lose efficiency. Ultimately, 200 L of final effluent was successfully filtered, representing the 24 h WWTP outflow.

As for the activated sludge (4) and the centrifuge rejected water (5), samples were collected using a 1 L glass beaker and brought to the laboratory for extraction. Since these matrices are homogeneous and have an extended residence time in the WWTP, the sampling methodology applied can be considered sufficiently representative and consistent. The (4) and (5) samples were stored in a glass beaker with a metal lid, at 4 °C and in the dark until further processing for MPs extraction. Apart from the WWTP final effluent (3), all other samples were screened at 5000 μm using a stainless-steel sieve. If present, material > 5000 μm was inspected and any retained mesoplastics particles were collected and placed in glass Petri dishes for future analyses of organic and inorganic contaminants associated with plastics (data not published). **Appendix A Table S1** shows the volumes collected for each sampling point.

2.4. Microplastic extraction protocol

After sampling, the liquid remaining in the filter housing of (1), (2), and (3) samples were filtered through a tailored 1 μm stainless-steel fabric (Bopp®, Switzerland) and the retained material was transferred in a glass container. To promote the oxidation of most of the OM, the cartridge filter, along with 100 mL of 30 % H_2O_2, was transferred in the same glass container (**Appendix A Fig. S1**). To further improve the removal of the solid particulate and the recovery of MPs adhered to the filter and the stainless-steel fabric, the glass container was placed in a low-intensity ultrasonic cleaner (USC), for three cycles of 10 min each. Care was taken to prevent the solution temperature from exceeding 40 °C. After USC treatment, the cartridge filter and the stainless-steel fabric were removed, and the solution was subjected to Fenton reaction, in which the OM is oxidised by the combination of H_2O_2 with a ferrous catalyst. A 20 mg/mL aqueous solution of $FeSO_4{\cdot}7H_2O$ was identified as optimal for degrading residual OM, as per Hurley et al. (2018) and Tagg et al. (2017). A peroxide-to-catalyst volumetric ratio of 2 was employed, meaning that 100 mL of 30 % H_2O_2 solution was mixed with 50 mL of the catalyst solution. Reaction conditions were carefully controlled, maintaining the temperature around 40 °C using an ice bath and adjusting the pH to 4 with small amounts of 2 mol/L NaOH or 1 mol/L H_2SO_4 as needed. These precautions were taken to avoid sample loss and preserve MPs integrity. The resulting wet peroxidation (WPO) solution was kept stirring at 40 °C for 24 h. Afterwards, the WPO solution was collected on a 1 μm stainless-steel fabric, and the filtrate was washed at least three times with UP water and then transferred into a 500 mL separating funnel containing enough (~300 mL) $ZnCl_2$ solution (ρ~1.8 g/cm^3). After 48 h, the settled material consisting of red sludge and inorganic particles was discarded, while the clean solution containing floating particles was filtered on a 1 μm glass fiber filter (GF/F, Whatman (Cytiva), United Kingdom) using a glass vacuum filtration system. The final filters were then placed in covered glass Petri dishes and stored in a desiccator until analysis. The $ZnCl_2$ solution was collected, filtered again through 1 μm stainless-steel fabric, and regenerated at ρ ~1.8 g/cm^3 for subsequent reuse (up to five times).

For samples (4) and (5) (Fig. 1), a 100 mL sub-sample was taken, as this volume was deemed sufficient for WPO, given that sewage sludge is known to be rich in MPs (Bayo et al., 2016). The sub-sample was settled overnight, then the clear upper layer was directly filtered through a 1 μm stainless-steel fabric. Few drops of H_2O_2 were added to the filter to degrade OM and facilitate filtration. The material retained on the filter was then combined with the settled solids, and the entire mixture underwent the MPs extraction process. Specifically, 100 mL of 30 % H_2O_2 were added to the solids, and the beaker was treated in a low-intensity USC for three cycles of 10 min each. The resulting solution was subsequently processed via the Fenton reaction, followed by density separation using zinc chloride, as previously described. **Appendix A Fig. S2** shows the sample purification procedure used in this study, differentiating between samples collected through the stainless-steel cartridge filtration, and samples grabbed in glass beakers (activated sludge and centrifuge rejected water). This procedure is based on widely used methods described in the literature (Masura et al., 2015; Mintenig et al., 2017; Tagg et al., 2017). The method was previously tested on a batch of standard MPs consisting in PVC, PET, PP and high-density polyethylene (HDPE) (**Appendix A Table S2**), with particle sizes ranging from 500 to 2000 μm. These MPs were subjected to the full extraction procedure, including USC, WPO, and density separation. The mass recovery rate exceeded 90 % for all polymers, with PP exhibiting the highest mass loss and PVC the least. Visual inspection of the treated particles under an optical microscope revealed no changes in their size and colour, indicating minimal physical or chemical alteration during the process.

2.5. MPs characterization and quantification

The dried filters were first analysed with a Fourier transform infrared spectroscopy microscope equipped with a FPA detector (Cary 620-670 FTIR microscope FPA detector, Agilent Technologies, Inc., USA), which allows 2D imaging-FTIR analysis of MPs directly on the filters. This analytical approach for the identification and counting of MPs has been widely used in literature (Cincinelli et al., 2017; Hendrickson et al., 2018; Roscher et al., 2022). Analyses were performed in reflectance mode with a spatial resolution of 4 cm^{-1}, acquiring 128 scans per spectrum. Each analysis focuses on a 700 × 700 μm^2 box (128 pixels × 128 pixels) and each pixel has a size of 5.5 × 5.5 μm^2 (spatial resolution of the imaging map of 5.5 μm). To reduce analysis time, as commonly done in MPs spectroscopy (Huppertsberg and Knepper, 2018), five 5-mm squares (each with an area of 25 mm^2) were randomly selected and analysed from the total 1134 mm^2 area of the filter (with an effective filtering surface of Ø = 38 mm). In this way, approximately 11 % of the total filter surface was analysed for each sample, enabling efficient analysis while ensuring a reasonable degree of accuracy within the limitations of the study. We assumed that the analysed MPs were representative of the material captured on the filter, i.e., evenly distributed, and we estimated the total number of MPs in the samples accordingly. For each identified polymer, a detailed description of the 2D FTIR imaging and specific absorption bands is provided in the supplementary data (**Appendix A Figs. S3-S11**). The colour of MPs was identified using FTIR-associated microscopic observations.

Being a non-destructive technique, once the FPA micro-FTIR analysis was completed, the filters were backwashed with 10 mL of absolute ethanol (EtOH VLSI, VWR) using a ceramic Buchner funnel connected to a vacuum pump. To maximise the recovery of MPs retained on the filter, the latter was subsequently immersed in approximately 10 mL of absolute EtOH, and the whole sample was sonicated for 20 s in low-frequency USC. The EtOH solution containing MPs was then refrigerated until LDIR analysis. LDIR analyses were carried out with an Agilent 8700 LDIR Chemical Imaging System, having hardware version LP3 and operating software Clarity 1.5.58. The wavelength range used for analysis is between 1800 and 975 cm^{-1}, and the instrumental performance is optimised for the analysis of MPs. For analysis, four 5 μL drops of the previously prepared MPs suspension in EtOH were placed on a clean slide, which was then transferred to the LDIR measuring chamber. This equates to a total of 20 μL, representing 0.1 % of the entire 20 mL solution, being analysed. To analyse representative aliquots of the bulk sample, immediately prior to taking the 5 μL from the test tube, the test tube was vortexed for 2 s (minimum r/min), and while the sample was taken, the test tube was kept shaking by hand shaking. As recommended by the instrument manufacturer, matching values above 0.80 were con-

sidered indicative of high-quality polymer identification. Like the approach used for FTIR analysis, three spectra were examined for each polymer in the LDIR analysis to verify the presence of polymer-specific diagnostic bands and confirm the accuracy of the results (See **Appendix A Figs. S12-S22**. An example is given for each polymer). After this confirmation test, some particles were rejected (unassigned spectra) even though their software matching was > 0.80, as some diagnostic bands identifying the chemical nature of the polymer were missing. The highly automated nature of LDIR significantly reduced the sample manipulation needed for analysis allowing the possibility to collect data even overnight.

The major aliquot of EtOH solution containing the MPs and not used for LDIR analysis was filtered on 1 μm glass fiber filter and analysed with TD-GC/MS. To be analysed directly, the filter was rolled up and placed in the sample tube (**Appendix A Fig. S31**), which was placed in the autosampler of the thermal desorber, and from there desorbed for GC/MS analysis. **Appendix A Table S3** summarises the instrument specifications and operating parameters settings optimised for the analysis of MPs. As a precaution, analyses were initially performed with a split of the desorbed analyte stream, analysing only 10 % of the total, to avoid signal saturation and possible clogging of the GC column. The remaining 90 % was collected on MARKES UNIVERSAL activated carbon vials, which are designed to capture C_2-C_{30} compounds. This gas split was done for the influent samples (1), activated sludge (4), and centrifuge rejected water (5). In the other samples, the split was lower (50 %, or 30 %) or nil, i.e., splitless analysis. For the construction of the calibration curve for the quantification of polymers in the samples, aliquots of naturally aged and degraded commercial polymer materials were used. The polymers investigated were those most found in the environment and in samples from WWTPs, namely PVC, PP, PE, PS, ABS, tires, PMMA, and bioplastic (Mater-bi). The choice not to use pristine MPs standards but aged and weathered commercial materials was made to obtain signals as similar as possible to those resulting from environmental plastics. Indeed, these MPs contain additives and impurities that could influence the analytical response of the thermal GC/MS, leading to different signals compared to pure standard polymers. Binary and ternary mixtures of these polymers were also analysed to evaluate the presence or absence of potential interferences between the signals of different polymers. Representative spectra of the polymers analysed using TD-GC/MS are shown in **Appendix A Figs. S23-S30**, while **Appendix A Table S4** lists the selected molecules for the identification and quantification of the polymers, along with other values such as retention time and main molecular weights.

The MPs size classification, in μm, was divided into >1000, 500–1000, 300–500, 50–300, and 10–50. A similar size classification was employed in the review by Ali et al. (2021). Due to the significant number of particles around 50 μm observed, this size range was specifically included. Various cellulose fibers (CFs) were identified in the samples. In the graphs, CFs will be categorized under MPs; however, their distinct characteristics will be addressed in the discussion. CFs that bypass WWTPs and enter aquatic environments can act as vectors for contaminants, much like MPs. Given their higher biodegradability compared to MPs, CFs may release associated contaminants more readily, underscoring their inclusion in this study. **Appendix A Table S5** provides details on the different CFs commonly found in wastewaters. To simplify data comparison, results from various methods are expressed as the number or mass of MPs per litre (MPs/L) of sample. Fiber dimensions were defined by their length, representing the longest dimension of the particle. Generally, the fibers found have small diameters (20-50 μm) and lengths ranging from a few hundred μm to several mm. For other particle types (fragments, granules, films), the longest side was also recorded as the size measurement. The FTIR classification of MPs into morphological classes followed the geometric criteria from Markley et al. (2024), with size manually measured using the instrument's internal tools. In contrast, LDIR automatically measured numerous structural parameters of each particle, and these measurements were combined with a visual inspection of images captured by the instrument to determine morphology. In this study, the (largest) particle size data will primarily be considered to facilitate comparison with results obtained from FTIR and LDIR spectroscopic techniques. Nevertheless, leveraging additional values from the LDIR analysis could yield valuable insights. For example, while it would require relatively strong assumptions for certain parameters characterising MPs, a model could be used to estimate the total polymeric mass of LDIR-detected MPs. The accuracy of this model could then be validated using spectrometric analyses, such as TD-GC/MS.

2.6. Quality assurance and quality control

Glass and stainless-steel instruments and containers were used whenever possible, each thoroughly washed three times with UP water. Strict precautions were implemented during sampling and analysis to minimize and monitor potential self-contamination, including the use of coloured lab coats and gloves. In the laboratory, sample preparation was conducted under a fume hood in a clean environment. To evaluate potential self- and cross-contamination, experimental blanks were prepared for each extraction step by exposing a beaker of UP water near the samples during processing. This water, along with all reagents used in the extraction, was filtered through a 1 μm glass fiber filter. Contamination levels were quantified by calculating the average contamination observed in the experimental blanks, which was then subtracted from the sample data to correct the results. The recovery efficiency of the method was assessed by applying the extraction procedures to samples spiked with MPs particles produced in the laboratory (section 2.4).

3. Results and discussion

3.1. MPs in the influent wastewater

As shown in Fig. 2**a**, the main polymer found in the influent wastewater detected by micro-FTIR analysis is PBR (60 %), followed by EVA (30 %). The MPs concentration in this matrix is 72 MPs/L. This value is consistent with that found in similar studies (Sun et al., 2019). As reported in Fig. 2**b**, most particles were found to range between 10 and 50 μm, followed by slightly larger particles ranging from 50 to 300 μm. Among the smallest particles (10 and 50 μm), only PBR and EVA were detected. However, a small number of particles of this polymer were also found in the size fraction larger than 300 μm. Fig. 2**c** and 2**d** shows that most particles entering the WWTP were granules, particularly small PBR granules (26 %). These MPs likely originate from street washing and pipe wear. Although the plant primarily treats wastewater from areas with white/black water separation, some areas still lack complete separation, allowing urban run-off to carry MPs worn from tires. The influent sample contained approximately 16 EVA films/L, with l film size ranging between 500 and 1000 μm. Additionally, a small quantity of relatively large PAN fibers (300-500 μm, 3 % of total fibers) and acrylate granules were found. The colour distribution of the MPs found in the influent sample was primarily transparent (EVA), followed by black (PBR), white (acrylate) and red (PAN). It is worth noting that, as mentioned in paragraph 1.5, only approximately 11 % of the filter from each sample was analysed, with the total MPs content extrapolated from these measurements. Therefore, the results obtained via micro-FTIR may not provide a complete overview of the actual sample composition. The presence of other polymers in the influent sample cannot be ruled out. The relatively low number of fibers detected entering the plant is surprising, given that fibers are a major form of MPs in municipal wastewater (Lares et al., 2018), as will be shown by the identification of several fibers in other samples. Therefore, LDIR and TD-GC/MS analyses are essential to supplement the results obtained with micro-FTIR.

The concentration of MPs detected via LDIR is significantly higher with respect to FTIR analysis (**Appendix A Fig. S32**). Specifically, 2117 MPs/L were found in the influent compared to 72 MPs/L identified by micro-FTIR—an increase by a factor of 30. Most particles measured by

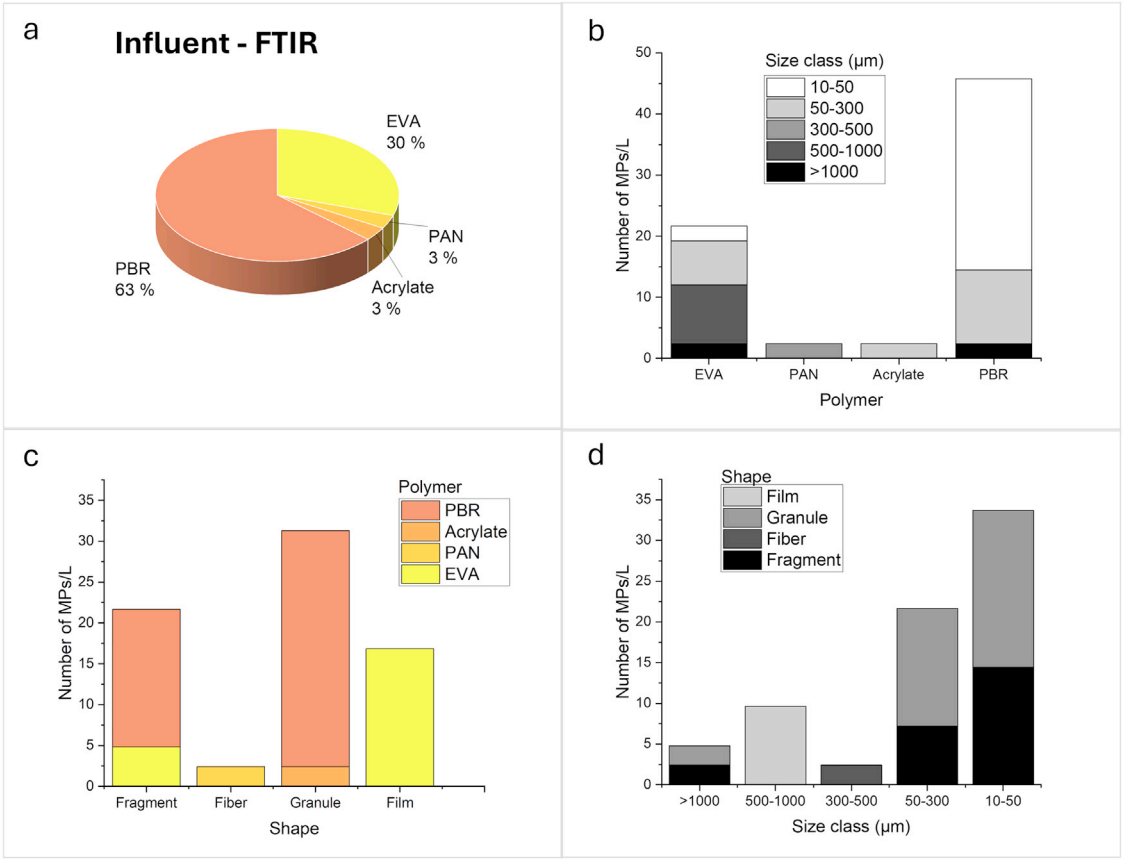

Fig. 2 – Focal Plane Array (FPA) micro-FTIR characterization of microplastics (MPs) found in the influent sample. The figure shows the abundance (%) of polymers in the sample (a), and the fractionation of MPs according to: Polymer type and size (µm) class (b); morphological characteristics and polymer type (c); morphological characteristics and size (µm) class (d). PBR: polybutadiene rubber; PAN: polyacrylonitrile; EVA: Ethylene vinyl acetate.

LDIR were in the smaller size classes (10-300 µm), with only 17 particles exceeding 300 µm in size. The disparity may stem from the sample preparation procedure, which involved using a micropipette (P20) with a very small tip opening, making it challenging to collect larger particles. LDIR offered a detailed analysis of each particle in the EtOH dispersion aliquot, providing comprehensive structural measurements (e.g., height, length, aspect ratio, perimeter, surface area, eccentricity, solidity) alongside chemical identification. In contrast, micro-FTIR analyses were conducted manually, with the operator selecting and analyzing each potential MPs particle individually. This approach was subjective and less effective in samples with high MPs concentrations, potentially leading to undetected particles. LDIR detected particles as small as 12 µm, surpassing micro-FTIR, which struggled with particles below 20 µm. LDIR enabled high-throughput analysis, including overnight operation. While FTIR required continuous operator involvement, it offered a broader spectral range and greater reliability compared to LDIR. Notably, LDIR can detect particles as small as 5.5 µm in reflectance mode and down to 1 µm in attenuated total reflection mode (Laskar and Kumar, 2019). However, FTIR instruments operate within a spectral range of 900 to 3000 cm^{-1}, whereas LDIR systems are limited to a narrower band of 1800 to 975 cm^{-1}. To facilitate the discrimination of particles using the FPA micro-FTIR, it would have been possible to dilute the sample or perform a more aggressive chemical treatment to better remove the OM. However, this approach could cause alteration of the plastic polymers and hinder their identification. Another option could involve the use of sequential cartridge filters, which allow for the preselection of microplastics based on their sizes. For instance, a series of cartridge filters could be installed on the sampling system, with a nominal pore size of 300, 10 and 2 µm.

2.2. MPs removal in primary treatments

In this case, as reported in Fig. 3**a**, most MPs identified through micro-FTIR analysis consisted of PBR and EVA, although PET fibers represented 22 % of the total polymers. In the effluent of the primary clarifier, a concentration of 32 MPs/L was found, including 2 CFs. The MPs removal during these primary treatments, which include coarse screening, oil and grease separation, and primary sedimentation (Fig. 1), was approximately 55 %, a value consistent with findings in the literature (Ali et al., 2021). Initial screening and grit removal eliminate larger MPs, while aeration during grease removal creates air bubbles that allow smaller particles to rise and be skimmed off. During primary sedimentation, processes like surface skimming, gravity separation, and sorption remove heavy MPs and those trapped in solid flocs. Chemicals such as ferric sulphate and flocculating agents further enhance MPs removal by promoting the aggregation of suspended particles (Rout et al., 2022). Comparing the MPs content at this purification stage with that in the influent, it is evident that PET, PP, and CFs were absent in the influent but present in the sample collected after primary sedimentation (Fig. 1). This discrepancy may be attributed to the autosampler not capturing wastewater aliquots containing these polymers. Alternatively, these polymers, absent at the influent sample, could originate from the centrifuge rejected water (sludge dewatering), which is reintroduced into the system upstream of the primary clarifier (Fig. 1). Most MPs found after the primary treatment had sizes ranging between 50 and 300 µm, followed by those between 300 and 500 µm, and 10-50 µm (Fig. 3**d**). Among the 10-50 µm particles, only PBR was found. However, particles of this polymer were not found in the size fraction larger than 300 µm. This could be because larger PBR particles were removed through flocculation-

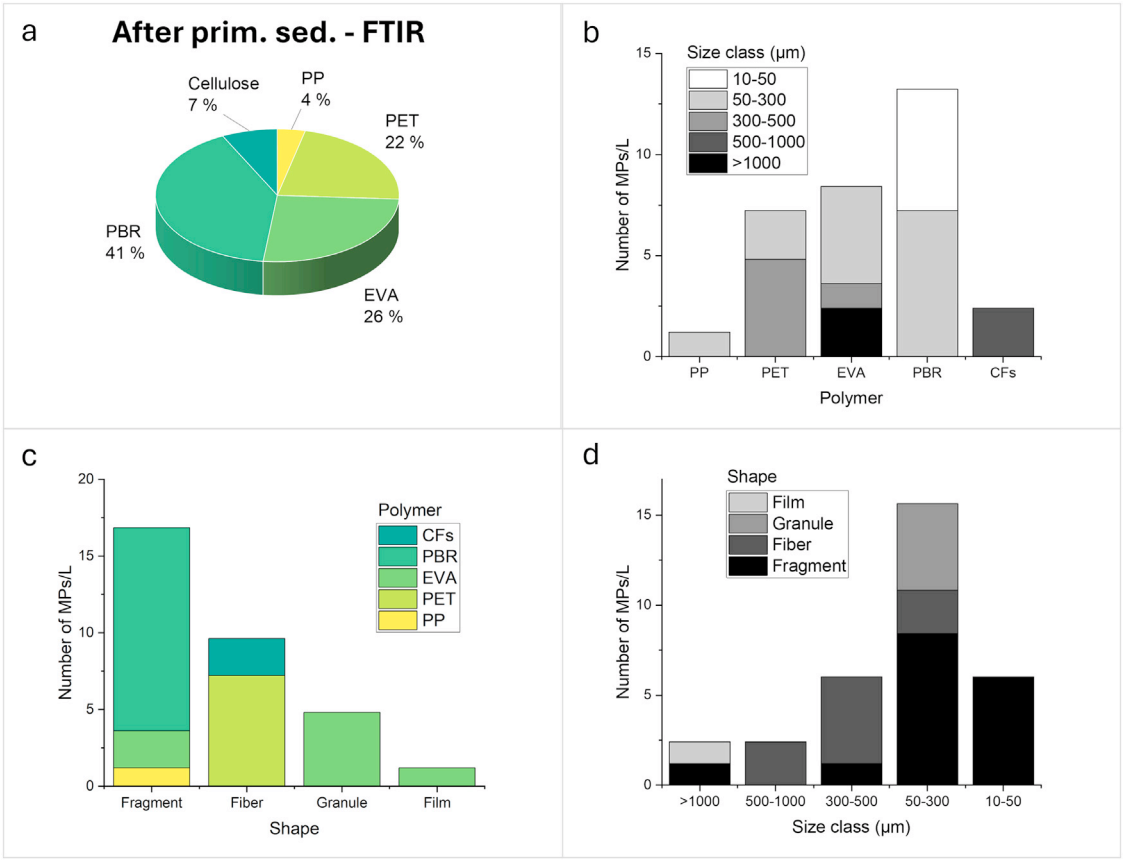

Fig. 3 – FPA micro-FTIR characterization of microplastics (MPs) found in the primary clarifier effluent sample. The figure shows the abundance (%) of polymers in the sample (a), and the fractionation of MPs according to: Polymer type and size (µm) class (b); morphological characteristics and polymer type (c); morphological characteristics and size (µm) class (d). PP: polypropylene; PET: polyethylene terephthalate; CFs: cellulose fibers.

coagulation-sedimentation during the primary treatments, thus ending up in the primary sludge. EVA and CFs particles were the one with larger sizes, namely > 500 µm (Fig. 3**b**). However, the quantity of large particles (> 500 µm) found after primary treatments was significantly lower compared to the number of small-sized particles. This is confirmed in the literature, where primary treatments are proven to be effective in removing larger MPs particles. For example, Dris et al. (2015) observed a significant reduction in the fraction of large particles (1000-5000 µm) from 45 % to 7 % after primary sedimentation. As seen in Fig. 3**c** and **d**, most particles found in the primary clarifier effluent were fragments (53 %), particularly fragments of PBR ranging in size between 50 and 300 µm (25 %) and between 10 and 50 µm (19 %). Additionally, PET and CFs, predominantly larger than 300 µm, accounted for 31 % of the total MPs. Among the major uses of PET are fibers for clothing, and containers for liquids and food (Geyer et al., 2017). That is the reason why it is commonly found as fibers in WWTP samples. The EVA granules constituted 16 % of the total MPs in the primary clarifier effluent, with sizes ranging between 50 and 300 µm. Films represented the smallest fraction of MPs found (3 % of the total) and had sizes exceeding 1000 µm. The MPs in the primary clarifier effluent were primarily black (PBR, PET), followed by white (EVA), transparent (EVA), and blue/green (PP). It is important to note that not all particles scanned via FTIR were included in the results, as some FTIR spectra were indecipherable, including those of conglomerates of black and magenta particles.

The MPs concentration measured via LDIR in samples from the effluent of the primary clarifier was 944 MPs/L (+28 CFs) (**Appendix A Fig. S34**). Comparing this data with the MPs count in the influent sample, the removal attributed to the primary wastewater treatment and measured with LDIR was 54 %, in agreement with the FTIR analysis (55 %) and consistent with literature data (Enfrin et al., 2019). Most MPs identified were classified as "Rubber" (49 %), followed by PP (28 %), PU, and ABS (6 %). FTIR analyses highlighted a high presence of PBR in the samples, which could correspond to the "Rubber" identified in LDIR (see diagnostic bands in **Appendix A Fig. S22**). It is worth to note that both these techniques detected polymers such as PET, PP, and CFs, even if EVA particles were detected only by FTIR. Once again, the particles identified via LDIR are predominantly in the size classes < 300 µm. Similarly to FTIR findings, the most abundant MPs detected by LDIR were fragments, followed by granules and films (**Appendix A Fig. S33c and d**). However, the quantity of identified fibers was very low (less than 3 %), contrasting with FTIR results, where fibers accounted for 25 % of the sample. This discrepancy suggests that the LDIR instrument may struggle to accurately analyse fibers in samples with high particle density, as observed in this case.

3.3. MPs leaving the WWTP through the effluent

As reported in Fig. 4**a**, the most abundant polymer found in the WWTP effluent is EVA, followed by PS, neoprene, CFs, and PE. Considering a 200 L sample volume, the concentration of MPs and CFs in the WWTP effluent was 1.05 MPs/L. This value aligns with measurements from similar plants using analogous analytical techniques (Sun et al., 2019). Consequently, the MPs removal efficacy of the investigated plant is approximately 98 %. Such high efficiency, even for a conventional treatment plant, may be influenced by the size of the WWTP. This plant, designed to treat 450,000 pe, typically handles only about half of its intended capacity. As a result, the coagulation, flocculation, and sedimentation processes could be particularly effective. Interestingly, the chemical composition of MPs detected in the influent differs from that in the WWTP effluent. The types of polymers identi-

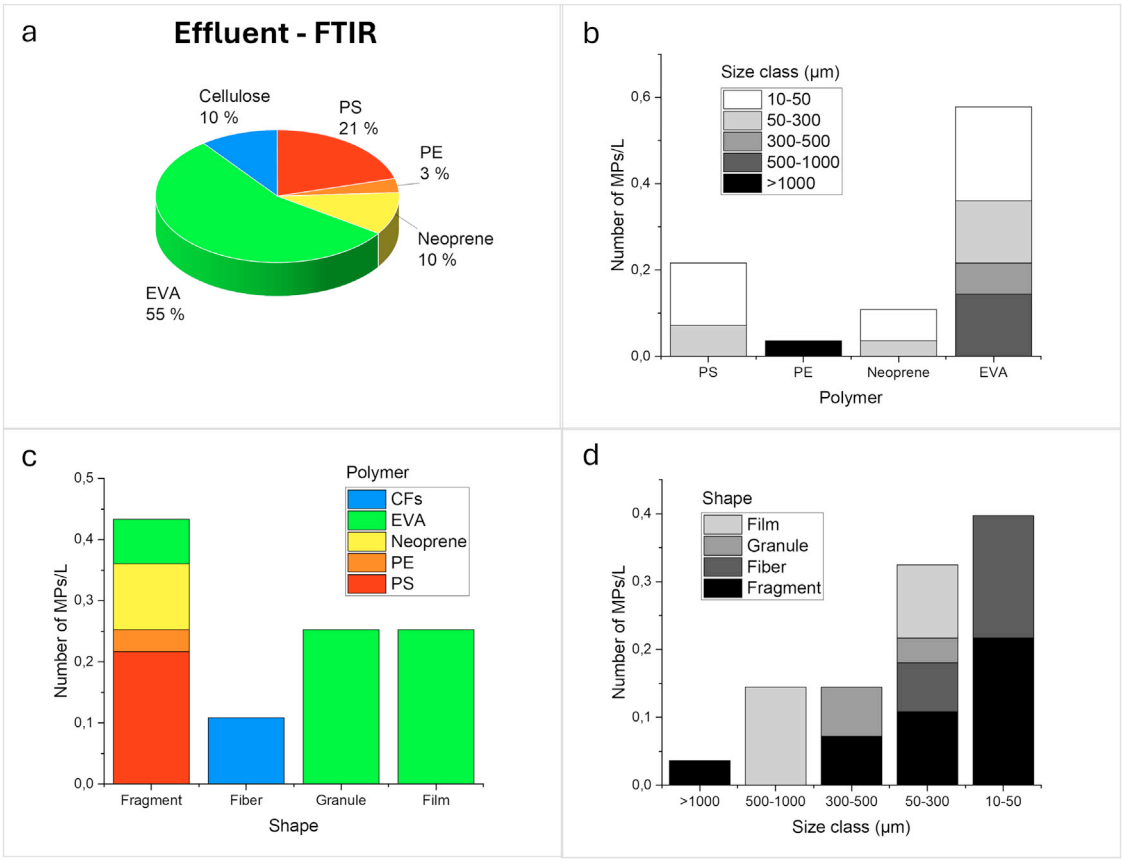

Fig. 4 – FPA micro-FTIR characterization of microplastics (MPs) found in the wastewater treatment plant effluent sample. The figure shows the abundance (%) of polymers in the sample (a), and the fractionation of MPs according to: Polymer type and size (µm) class (b); morphological characteristics and polymer type (c); morphological characteristics and size (µm) class (d). PE: polyethylene; PS: polystyrene.

fied change across treatment stages, highlighting the complex and unpredictable dynamics of MPs within WWTPs. These findings underscore the importance of comparing different analytical techniques to evaluate whether one method provides more consistent and reliable results than others. As can be seen in Fig. 4**c** and 4**d**, most MPs exiting the plant were found to be fragments (41 %), particularly small-sized fragments of PS and neoprene (50-300 µm and 10-50 µm, totalling 31 %). Several EVA fragments found in the effluent were granular or film-shaped, with size ranging from 500 to 1000 µm. The investigated WWTP operates as a conventional activated sludge plant without tertiary filtration or advanced technologies for further removing contaminants and suspended solids. Literature suggests that implementing final filtration methods, such as disc or sand filtration, could significantly improve the removal of large MPs (Talvitie et al., 2017b). The fibers identified in the WWTP effluent were CFs, constituting approximately 10 % of the total MPs in the effluent, with most ranging from 300 to 500 µm in size. While cellulose is biodegradable by environmental organisms, its potential environmental impact remains significant. Similar to MPs, cellulose microparticles can act as carriers for potentially toxic chemicals, emphasizing the need for further investigation and mitigation strategies. The MPs colour in the WWTP effluent sample was mainly transparent (EVA, PS), white/blue (EVA), black (neoprene, CFs), and blue (PE). It is noteworthy that several reticulated-shaped EVA fragments were found. These fragments were identified not only in the effluent but also in the influent sample, as well as in the sample collected after the primary clarifier.

Even for the WWTP effluent, the LDIR analyses measured a concentration of MPs (93 MPs/L) that is much higher than the concentration found with micro-FTIR analysis (1 MPs/L). LDIR enabled analysis at a spatial resolution of up to 5.5 µm, with a pixel size range as small as 1 µm in reflection mode. Although the spatial resolution of FPA micro-FTIR was comparable (pixel size of 5.5×5.5 µm^2), analysing MPs smaller than 20 µm with FPA micro-FTIR proved challenging since only few spectra (2-3) are collected on such samples, with no reliable statistics on spectral features (e.g., diagnostic bands, oxidation peaks). It is important to note that while the LDIR analysis was fully automated (section 2.5), the manual FTIR analysis may have led to an underestimation of the particles present on the filter. However, the LDIR instrument only provides spectra in the fingerprint region, which can pose challenges in identifying altered or aged MPs. The FPA detector used in micro-FTIR has a sensitivity of <0.5 pg/pixel, sufficient to detect plastic polymers on the glass fiber filter. Nonetheless, its lower spatial resolution and signal-to-noise (*S/N*) ratio compared to LDIR require multiple scans (e.g., 128 or more) to achieve high *S/N* spectra when analyzing MPs samples mixed with sediment or organic/inorganic materials. In the absence of interferences, fewer scans are needed, enabling faster measurements and the ability to scan larger filter areas. The main advantage of FPA micro-FTIR lies in its ability to confirm polymer identification with greater accuracy by analyzing the full mid-IR spectral range. In contrast, LDIR excels in time efficiency for screening filters crowded with numerous plastic particles. Using these methods in tandem provides a more comprehensive analysis, combining the precision of FPA micro-FTIR with the speed and efficiency of LDIR. Nevertheless, the calculated MPs removal efficiency of the WWTP using LDIR data was around 96 %, comparable to the 98 % obtained using FTIR data. The MPs measured with LDIR in the WWTP effluent were smaller than 300 µm, with the majority ranging between 10 and 50 µm (**Appendix A Fig. S34**). Of these MPs, 65 % were fragments, primarily composed of Rubber, as well as PP and polyoxymethylene (**Appendix A Fig. S34c and d**). An additional 18 % were films (PP and PU), while only 7 % were fibers (polyamide (PA) and PU).

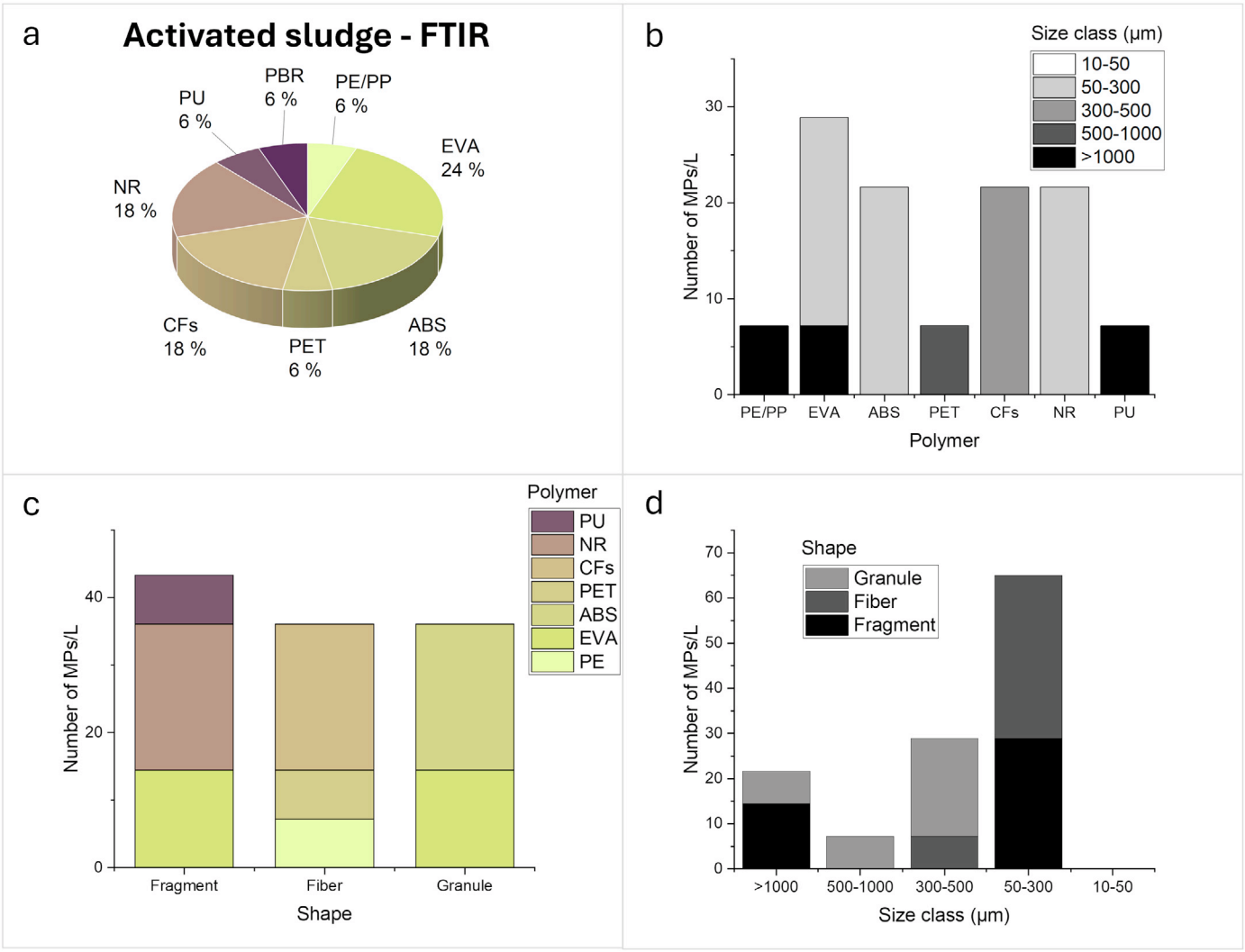

Fig. 5 – FPA micro-FTIR characterization of microplastics (MPs) found in the activated sludge sample. The figure shows the abundance (%) of polymers in the sample (a), and the fractionation of MPs according to: Polymer type and size (µm) class (b); morphological characteristics and polymer type (c); morphological characteristics and size (µm) class (d). PU: polyurethane; NR: nitrile rubber; ABS: acrylonitrile butadiene styrene.

3.4. MPs trapped in the activated sludge

The number of MPs detected in the activated sludge, 123 MPs/L, was significantly higher than in previous samples. Among these MPs, 18 % were classified as CFs. The identified polymer classes in the activated sludge were diverse (Fig. 5), as was the particle size distribution. Approximately 53 % of MPs ranged between 50 and 300 µm, while the remaining particles were between 300 and over 1000 µm. FPA micro-FTIR analysis revealed that EVA was the most abundant polymer in the sludge, followed by nitrile rubber (NR), ABS, and cellulose. As shown in Fig. 5**c** and **d**, most of the MPs identified were fibers of PET and cellulose, ranging in size from 50 to 300 µm (30 %), followed by fragments within the same size range (24 %). In this matrix, PU fragments were also detected. PU is widely used to create elastic materials for applications such as seals, soft parts of toys, clothing and accessories, and medical products. Additionally, it is commonly used in paints and adhesives. Fragments of NR were also found. The MPs inspected in activated sludge samples were primarily red or reddish in colour (PET, PE, CFs, NR), followed by white (PU, ABS, PBR), black (CFs), green (EVA), and blue (EVA). No films were detected in the activated sludge. The concentration of MPs in activated sludge was therefore nearly double that of the influent and approximately twelve thousand times higher than the concentration in the effluent (FTIR data). Not all particles were analysed, as the FTIR spectra of some scans were too noisy to be clearly attributed. These included numerous large black conglomerates (> 500 µm) and green fragments (> 500 µm) with a 'net-like' structure.

With a total solids content of 5.56 g/L, it is estimated that one kg of dry activated sludge contains over 200,000 MPs. These results demonstrate that activated sludge retains a high concentration of MPs, suggesting their accumulation within the sludge line of WWTPs. Sludge flocs and extracellular polymeric substances secreted by biomass in aeration tanks play a significant role in capturing MPs, which subsequently settle in secondary clarifiers. Additionally, MPs can be ingested and retained by protozoa and metazoa (Kanold et al., 2021). Prolonged contact times in biological treatment promote biofilm formation on MPs surfaces, altering their physicochemical properties and improving removal efficiency. These processes, in combination with factors such as polymer type and operational conditions, are critical for the effective removal of MPs (Jani et al., 2024). MPs, particularly those that are degraded, porous, and rough, can serve as growth substrates for bacteria. This mechanism parallels the principle of Moving Bed Bioreactor (MBBR) technology, where plastic elements provide a physical surface for microbial biofilm growth that aids in the degradation of organic contaminants (Bassin and Dezotti, 2018). However, bacterial colonization on MPs can

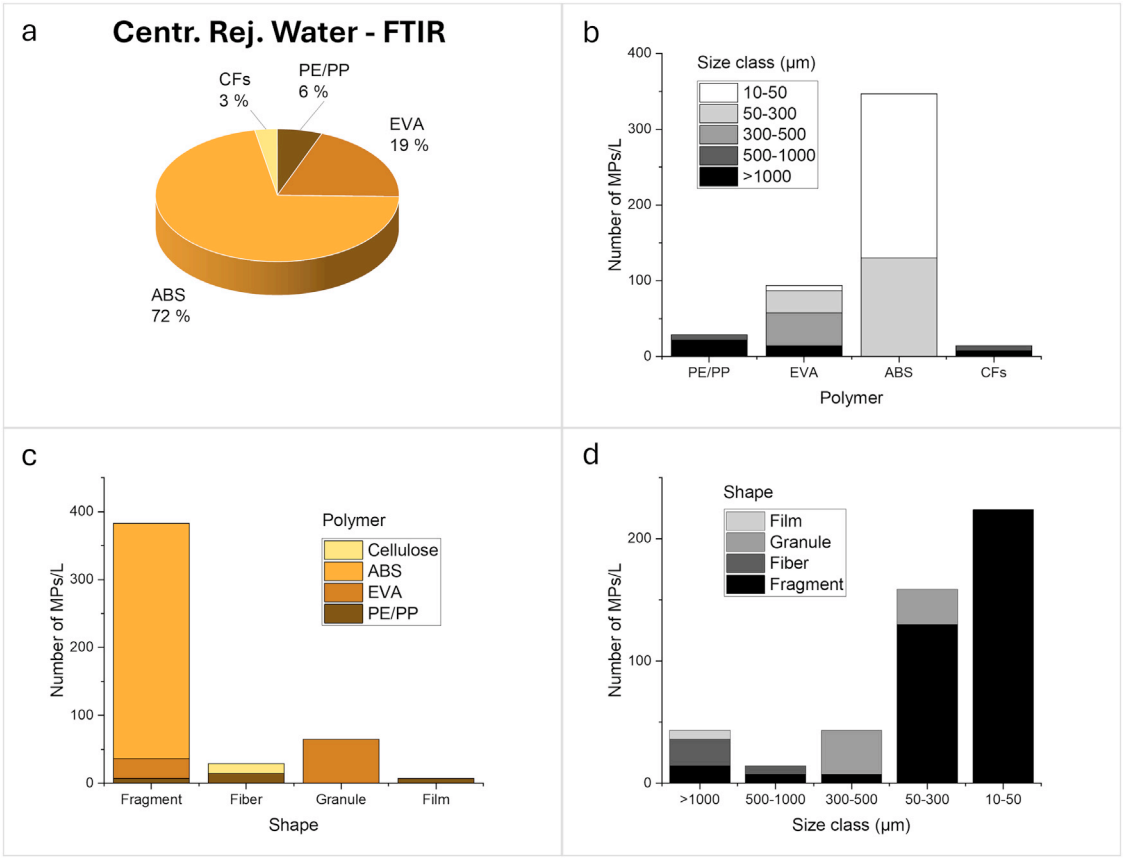

Fig. 6 – FPA micro-FTIR characterization of microplastics (MPs) found in water extracted during centrifugation sludge dewatering. The figure shows the abundance (%) of polymers in the sample (a), and the fractionation of MPs according to: Polymer type and size (µm) class (b); morphological characteristics and polymer type (c); morphological characteristics and size (µm) class (d).

modify their spectral profiles, complicating polymer identification via infrared spectroscopy. Despite these challenges, MPs may enhance oxidative biological treatment efficiency, though their environmental release must be minimized. Studies have shown that MPs negatively impact methane production during the AD of sewage sludge (Pittura et al., 2021). Moreover, prolonged exposure to chemical, physical, and biological degradation can fragment MPs into nanoplastics, which present an even greater environmental concern due to their smaller size and increased mobility.

In the activated sludge, the concentration of MPs measured with LDIR reached 10,800 MPs/L, much higher than the amount detected using FTIR analyses (almost 88 times). Most of the particles fell into the smallest size class (10-50 µm), followed by those in the 50-300 µm and 300-500 µm size ranges (**Appendix A Fig. S35**). The diversity of polymers found in the activated sludge samples was notable, with PU being the most prevalent, followed by PE, various Rubber, PA, ABS, and PET (**Appendix A Fig. S35a**). Notably, some of these polymers, including ABS, PE, rubber (PBR, NR), PET, and PU, were also identified during FTIR analyses. Both FTIR and LDIR analyses underscore the critical importance of effective sewage sludge management and disposal. Sewage sludge, encompassing activated sludge, primary sludge, and additional inputs from the sludge line, acts as the ultimate sink for MPs entering WWTPs. It also accumulates a wide range of emerging contaminants stemming from human activities, including pharmaceuticals, personal care products, and priority pollutants such as heavy metals and persistent organic pollutants (e.g., polycyclic aromatic hydrocarbons and polychlorinated biphenyls). In Italy and across Europe, composting disposed sludge is a common practice. However, applying this compost to agricultural soils introduces significant risks to human health and the environment. When composted sludge is used in agriculture, MPs and other non-degraded contaminants can irreversibly infiltrate the soil, ultimately entering human and animal food chains. Despite the potential benefits of sewage sludge for nutrient recovery, (e.g., nitrogen, phosphorous, and potassium), residual fractions should be prioritized for thermal destruction to mitigate these risks. If dewatered sludge contains a high concentration of MPs, energy recovery may present a viable disposal option. The specific heat values of most polymers (41.9–45.5 MJ/kg) are comparable to those of conventional fossil fuels, making sludge with high polymer content an efficient energy source (Cavazzoli et al., 2023). This approach aligns with circular economy principles while addressing the challenge of MPs contamination in agricultural applications.

3.5. Recirculation of MPs in the WWTP via centrifuge rejected water

FTIR analysis revealed that centrifuge rejected water samples contained the highest concentration of MPs, with 484 MPs/L detected, including 14 CFs. As shown in Fig. 6**a**, the predominant polymer was ABS, making up 72 % of the particles, followed by EVA (19 %), PE/PP (6 %), and cellulose (3 %). Most ABS particles were fragments in the smallest size fractions, specifically 10-50 µm and 50-300 µm. The sludge entering the centrifuge had already undergone AD and dewatering treatments (e.g., drying belts), which likely contributed to the high number of small MPs due to the fragmentation of larger particles. However, several particles larger than 1000 µm were also present (Fig. 6**b**), including 22 MPs/L of PE/PP, 14 MPs/L of EVA, and 7 CFs/L. In terms of colour, most MPs were black (ABS, CFs), followed by transparent (EVA, PP/PE, CFs), blue (EVA, PP/PE), and white (EVA). Black pigmented ABS pipes

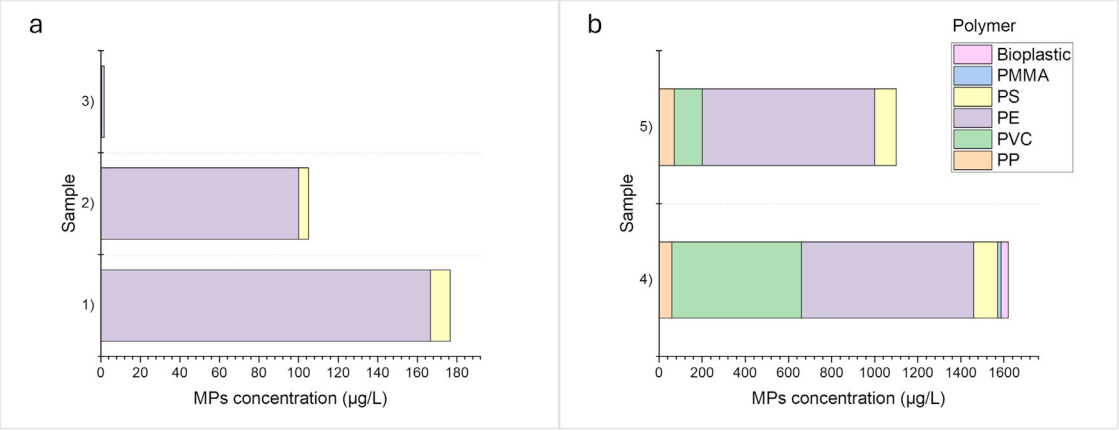

Fig. 7 – Thermal desorption gas chromatography coupled with mass spectrometry (TD-GC/MS) mass quantification of selected microplastic (MPs) polymers (PP, polyvinyl chloride (PVC), PE, PS, polymethylmethacrylate (PMMA), and bioplastic) in samples analyzed using FPA micro-FTIR and Laser Direct Infrared (LDIR). The figure illustrates the abundance of MPs ranging from 10 to 5000 µm in size, quantified in µg/L. Numbers represent sampling points: (a) 1) influent; 2) primary clarifier effluent; 3) wastewater treatment plant effluent. (b) 4) activated sludge; 5) centrifuge rejected water.

are commonly used in hydraulic applications. The numerous ABS fragments found in the centrifuge rejected water could be attributed to wear on these pipes within the system. In addition, urban run-off is another potential source of ABS particles, as this polymer has seen a significant increase in production across various manufacturing sectors over the past few decades (Jiang et al., 2020). ABS is highly susceptible to UV degradation (Henshaw et al., 1999); thus, if exposed to sunlight, such as in agricultural soils, it can degrade rapidly, releasing smaller particles and associated additives into the environment. The centrifuge rejected water is recirculated to the head of the plant, causing MPs to predominantly re-enter the sewage sludge. ABS has a slightly higher density than water (ρ_{pure} polymer = 1.04–1.12 g/cm^3), biofouling likely facilitates the coagulation and sedimentation of these particles. As a result, ABS accumulates in the sludge, driven by its continuous release from urban sources, degradation of the WWTP piping system, and the recirculation of centrifuge rejected water, which reintroduces ABS MPs into the wastewater line.

LDIR measurements revealed a concentration of 23,000 MPs/L (+500 CFs) in the water extracted from the centrifuge during sludge dewatering, which is approximately 50 times higher than the concentration detected through FTIR analysis. As reported in **Appendix A Fig. S36a**, the predominant polymers identified with LDIR were Rubber (34 %), ABS (23 %), PP (17 %), and PU (13 %). Little amounts of PET, CFs, and PA were also detected. The ABS content measured by LDIR was lower than that reported by FTIR (34 % vs. 72 %). This discrepancy may stem from the randomly selected filter areas scanned during FTIR analysis, which could have captured regions with a non-uniform distribution and higher concentrations of ABS particles, potentially overlooking particles of other polymers. The representativeness of the sample and the accuracy of manual systems are critical considerations in MPs analysis, particularly for environmental samples with high levels of organic and inorganic matter. Most MPs analysed by LDIR were found in the size ranges of 50-300 µm, with smaller fragments being predominant (**Appendix A Fig. S36c and d**). However, PU and PP films and granules between 300 and 1000 µm were also detected. Consistent with FTIR findings, LDIR analysis identified small fragments as the most prevalent shape of MPs in the centrifuge rejected water, followed by films (13 %), fibers (6 %), and granules (4 %). While the polymers identified using LDIR largely aligned with those found by FTIR, EVA was not detected, despite the LDIR database being updated with its specific spectrum. Notably, LDIR analysis identified a broader variety of polymers compared to FTIR, further highlighting the importance of using complementary analytical methods for comprehensive MPs characterization (**Appendix A Fig. S36**).

3.6. MPs mass quantification by TD-GC/MS

Compared to spectroscopic techniques, which indicated that centrifuge rejected water contains more MPs than other samples, TD-GC/MS analysis revealed a higher MPs mass concentration in the activated sludge (Fig. 7). Specifically, the analysis measured a total of 1620 μg_{MPs}/L in the activated sludge, equivalent to 291 µg/g or approximately 0.3 mg/g dw. While MPs account for only 0.03 % of the total activated sludge mass, it is essential to consider that submicrometric plastic particles have a minimal specific weight. PE emerged as the most abundant polymer across the various samples, followed by PVC, PS, PP, bioplastic, and PMMA. No detectable traces of MPs were found in the extraction blanks.

In the WWTP influent, the most prevalent polymers are PE and PP, with smaller amounts of PVC, PS, and PMMA. During primary sedimentation, the concentration of MPs decreases significantly, from 177 µg/L in the influent to 105 µg/L in the primary clarifier effluent, corresponding to a 41 % removal rate (Fig. 7). This reduction is consistent with findings reported in the literature but is lower than the reductions observed with FTIR and LDIR. It is important to note that TD-GC/MS analysis targets only specific polymers, which limits direct comparison with the other techniques that detect a broader range of compounds. In the WWTP effluent, the total concentration of MPs decreases significantly, particularly for polymers such as PVC, PS, and PMMA, while bioplastics were not detected. The concentration drops to 2 µg/L, representing a 99 % removal of MPs between the influent and effluent. As anticipated, the activated sludge sample exhibits the highest concentration of MPs, with PE being the most abundant polymer, followed by PP, PS, PMMA, and bioplastics. This high MPs mass concentration highlights the role of activated sludge as a significant sink and reservoir for MPs. The centrifuge rejected water contains substantial amounts of MPs (1100 µg/L), corroborating results from FTIR and LDIR analyses. As illustrated in the WWTP schematic (Fig. 1), water extracted during sludge centrifugation is redirected to the system before primary sedimentation. If the MPs in this water bypass purification and sedimentation processes, they could eventually end up in the effluent and, subsequently, in the environment. To address this, implementing effective treatment technologies for the centrifuge extracted water prior to recirculation within the plant is essential.

Unlike the FTIR and LDIR analyses, ABS and tire wear particles could not be identified using TD-GC/MS. The inability to analyze thermal degradation products of tire wear may be attributed to the thermal desorber's maximum operating temperature of 400°C, which is insufficient to effectively volatilize rubbers, as these materials are specifically de-

signed to withstand higher temperatures (Peters, 2002). Employing a pyrolizer (Py-GC/MS) that operates up to 900 °C may enhance the detection of compounds like ABS and tire wear particles. However, such high temperatures increase the volatility of many substances, potentially resulting in the formation of contaminated gases with degraded products. Furthermore, Py-GC/MS instruments typically have a sample size limit of 5 mg, which poses challenges in obtaining a sufficiently representative and analysable sample (Hermabessiere et al., 2018). The analytical method used in this study offers an advantage by enabling the direct analysis of the glass filter on which all MPs from environmental (WWTP) samples were collected, eliminating the need for additional intermediate processing steps. When analysing MPs using GC/MS, it is crucial to identify specific marker fragments for accurate polymer identification and quantification. Polymers such as PS, ABS, and tire wear particles share common thermal degradation products, like styrene and vinyl cyclohexene, making it challenging to quantify a specific polymer based solely on these shared fragments. To resolve this, additional complementary molecules should be investigated, such as mercaptans for tire wear fragments. In our analysis, no thermal desorption products indicative of ABS or tire wear were detected, so these polymers were not considered present in the samples. Following methodologies used in other studies, benzene was selected as a marker for quantifying PVC content in the samples (Dehaut et al., 2016; Fischer and Scholz-Böttcher, 2017). However, the presence of benzene in the samples may not be exclusively due to PVC, demanding a more selective and specific marker. However, the presence of benzene in the samples may not be exclusive to PVC, highlighting the need for a more selective and specific marker. For PS quantification, styrene was chosen as the fragmentation product. Although styrene is also present in ABS and tire wear particles, it was attributed solely to PS because other identifying fragments—such as benzene-butane nitrile for ABS and mercaptans for tires—were not detected. While it is reasonable to attribute the styrene fragment to PS, there remains a possibility of some contribution from other polymers. The variability of polymers in the environment complicates instrument calibration for MPs quantification. For instance, laboratory tests on PET MPs using TD-GC/MS revealed that particles of the same polymer but different colours produced significantly different chromatograms (data not shown). This variability makes establishing precise chromatographic references for specific polymers a lengthy and complex process. Additionally, mixtures of different polymers, which are present in all environmental samples, generate new reaction by-products during the thermal desorption phase. These by-products create additional peaks that must be interpreted. For example, the chromatograms of PET and PVC analyzed separately differ from those of a PET and PVC mixture analyzed in the same run (data not shown).

3.7. Calculation of MPs removal efficiency and environmental emission factors

This paragraph discusses the emission factors associated with the studied WWTP in relation to the LDIR and TD-GC/MS results. LDIR detected the highest number of MPs and is therefore considered to provide the most conservative estimates of environmental emission factors. In contrast, TD-GC/MS provides complementary data by measuring the emitted mass of the investigated polymers (PP, PVC, PE, PS, PMMA, bioplastic). For details on the WWTP data used to calculate MPs removal and emission factors, please refer to **Appendix A Tables S6-S10** (Supplementary data). Given that the sampling method used in this study did not capture MPs in the 1–10 μm size range, the following calculations are likely underestimating the total MPs released into the environment. The estimation of MPs emission factors attributable to the investigated WWTP was based on the total volume of treated wastewater (see section 2.1 - Materials and methods). CFs were excluded from these calculations.

LDIR analysis revealed that the influent wastewater contained 2117 MPs/L, equivalent to approximately 9×10^{10} MPs per day, predominantly ABS, PU, and rubber particles smaller than 300 μm. TD-GC/MS analysis indicated a total MPs concentration of 177 μg/L, corresponding to 7.5 kg/day, with over 94 % being PE and the remainder PS. Based on the WWTP's capacity of 337,000 pe, emissions were estimated at 265,687 MPs/(pe·day) (LDIR) and 22 mg_{MPs}/(pe·day) (TD-GC/MS). After primary sedimentation, MPs concentrations decreased to 944 MPs/L, reflecting a 54 % removal efficiency (η_{rem}). This reduction resulted from physical and chemical processes like sedimentation, flocculation, and skimming, particularly affecting MPs in the 50–100 μm range (η_{rem} = 62 %). Granules were removed most effectively (η_{rem} = 67 %), while films showed minimal removal (η_{rem} = 5 %). ABS and PU were removed with high efficiencies (η_{rem} = 93 % and 90 %, respectively), whereas rubber removal was limited to 9 %. TD-GC/MS analysis indicated a total MPs removal efficiency of 39 %, lower than LDIR findings most likely due to fewer analyzed polymers. PE concentrations dropped by 40 %, and PS exhibited a η_{rem} of 49 %. In the WWTP effluent, LDIR detected 4×10^9 per day (11,700 MPs/(pe·day)), mostly rubber and PP fragments under 300 μm. Assuming the effluent flow equalled the influent, biological oxidation achieved 90 % removal of MPs entering the tank, contributing to an overall η_{rem} = 96 %. This treatment effectively removed smaller MPs and films, which were less impacted during primary treatments (η_{rem} = 88 %). PET fibers, minimally reduced during primary treatments (η_{rem} = 13 %), were fully eliminated during biological oxidation and final clarification. TD-GC/MS identified all six polymers in the effluent (PP, PVC, PE, PS, bioplastic, PMMA) at a total concentration of 1.77 μg/L, equating to 75 g/day (0.22 mg_{MPs}/(pe·day)). PE accounted for 53 g, PVC 11 g, PP 6 g, PS 4 g, bioplastics 0.8 g, and PMMA 0.4 g. Although these values are modest compared to the total suspended solids (TSS) emissions of the WWTP (4 mg/L, approximately 169 kg_{TSS}/day), they may represent only part of the total MPs output. MPs in effluents can adsorb and transport contaminants like heavy metals, pharmaceuticals, and synthetic musk fragrances, and may carry microorganisms, viruses, or antibiotic resistance genes, posing significant environmental risks (Galafassi et al., 2021; Kirstein et al., 2016; Viršek et al., 2017). To minimize MPs emissions, advanced treatments like tertiary filtration, phytoremediation, or advanced oxidation processes should be implemented (Abi Farraj et al., 2024; Kim et al., 2022; Sarti et al., 2024). These technologies can enhance removal efficiency and mitigate associated risks, ensuring safer effluent discharge into the environment.

As previously discussed, calculating environmental emission factors for WWTPs must include not only the treated effluent but also the sludge produced and disposed of by the plant. Sewage sludge, frequently composted and applied to agricultural land, represents a significant pathway for MPs introduction into terrestrial environments. Research has demonstrated that sludge application markedly increases MPs accumulation in soils, with plastic loads steadily rising with successive applications (van den Berg et al., 2020). This trend underscores the long-term contamination risk posed by sludge-derived MPs, particularly as these particles persist and potentially fragment further in the environment. Sludge treatment processes may further alter MPs properties, such as surface area and chemical composition, influencing their environmental behaviour and improving pollutant adsorption and bioavailability, thereby posing risks to ecosystems and food safety (Hatinoğlu and Sanin, 2021). The accumulation of MPs in agricultural soil also raises concerns about their transport across the soil-water-plant continuum and potential entry into the food chain (Corradini et al., 2019). In this study, the MPs content in the final dewatered sludge was not directly measured. However, an estimate of this value was made using data provided by the plant operator, along with a mass and flowrate balance (**Appendix A Table S6**). Based on the LDIR results, the activated sludge contained 10,800 MPs/L, while the mass concentration was 1.6 mg_{MPs}/L (TD-GC/MS). From the mass balance calculations, it was estimated that the excess sludge produced, dewatered, and disposed on the specific sampling day contained 8.6×10^6 MPs per kg dw, or 0.75 g_{MPs}/kg dw (TD-GC/MS). These figures are concerning, especially as the MPs tar-

geted in this study were larger than 10 μm, suggesting that the actual content may be underestimated. These findings underscore the urgent need for comprehensive risk assessments and sustainable management of sludge reuse to address its environmental and health impacts. Another concern is the high concentration of MPs detected in the water extracted from the centrifuge, as all analytical techniques employed in this study reported elevated levels. With excess sludge undergoing dewatering and a centrifuge capture efficiency of approximately 90 %, the extracted water amounts to 447 m^3/day. According to LDIR measurements, each litre of this water contains approximately 22,500 MPs, predominantly rubber (34 %), ABS (23 %), PP (17 %), and PU. This translates to around 1×10^{10} MPs being reintroduced into the wastewater treatment line daily, equivalent to 11 % of the MPs entering the plant with the raw wastewater. TD-GC/MS analysis suggests that about 0.5 kg of MPs are returned to the treatment line daily (7 % of the mass of investigated MPs entering with the raw wastewater), primarily PE. However, the inability of TD-GC/MS to identify rubber and ABS, as indicated by LDIR results, suggests that the actual MPs load may be considerably higher. These findings align with previous studies (Salmi et al., 2021), which also reported significant reintroduction of MPs *via* centrifuge rejected water (Fig. 1). To mitigate this issue, it is strongly recommended to implement solutions that address this internal recirculation challenge, such as integrating filtration systems or an intermediate sedimentation step before reintroducing the extracted water into the treatment line.

Our findings contribute to the growing understanding of MPs pollution, emphasizing the role of WWTPs as significant sources of ecosystem contamination and potential human exposure. The adverse effects of MPs on aquatic organisms are well-documented, and emerging clinical evidence suggests possible health risks to humans, though the long-term implications remain unclear (Pal et al., 2024). This study supports global efforts to address and mitigate the environmental and health challenges posed by MPs (Giarrizzo et al., 2019), underlining the urgent need for appropriate treatment technologies and sustainable management practices to reduce MPs emissions.

4. Conclusions

Controlling plastic emissions is vital due to their substantial impacts on environmental and human health. Standardizing methods for sampling and analysing MPs, particularly particles as small as 1 μm, remains a key challenge. This study demonstrated the effectiveness and limitations of multiple analytical techniques in assessing MPs pollution in WWTPs. LDIR enabled efficient detection and quantification of MPs as small as 12 μm, offering high-quality, automated results with reduced operator error, though manual verification remains advisable for aged and weathered MPs. FPA micro-FTIR provided complementary data but faced challenges with particles smaller than 20 μm, with longer analysis times and potential operator-related biases for MPs-rich samples. TD-GC/MS complemented these findings by quantifying the mass of targeted polymers, though it required precise calibration and expert interpretation. Despite differences in analytical outputs, all methods revealed consistent trends in MPs behaviour and removal efficiency across the wastewater treatment processes. Conventional activated sludge treatments achieved over 96 % MPs removal, yet the large volumes of treated water still released significant MPs loads into the environment (4 billion MPs/day or 75 g_{MPs}/day, depending on the analytical method). MPs were predominantly retained in sewage sludge, underscoring the importance of sustainable sludge management to prevent their reintroduction into ecosystems *via* agricultural reuse. Energy recovery strategies, such as incineration or co-pyrolysis, could safely eliminate MPs while valorising sludge, aligning with circular economy principles by turning waste into a resource. Furthermore, centrifuge rejected water was identified as a significant pathway for reintroducing MPs into the wastewater treatment process. Effective interventions, such as filtration or intermediate sedimentation, are needed to intercept these particles before recirculation. By addressing these internal contamination pathways, WWTPs can further enhance MPs removal and reduce environmental emissions. Additionally, the adsorption properties of MPs present opportunities for removing micropollutants, offering a dual benefit for improving wastewater treatment efficiency. These findings highlight the critical role of WWTPs in mitigating MPs pollution and underscore the need for harmonized sampling and analytical methods to improve global monitoring efforts. Enhanced treatment technologies and sustainable sludge management practices are essential to minimizing environmental risks, protecting ecosystems, and supporting public health.

Declaration of generative AI and AI-assisted technologies in the writing process

During the preparation of this work the author(s) used ChatGPT in order to improve the language and readability of the manuscript. After using this tool/service, the author(s) reviewed and edited the content as needed and take(s) full responsibility for the content of the publication.

Declaration of competing interest

The authors declare that they have no known competing financial interests or personal relationships that could have appeared to influence the work reported in this paper.

CRediT authorship contribution statement

Simone Cavazzoli: Writing – original draft, Visualization, Methodology, Investigation, Formal analysis, Data curation, Conceptualization. **Costanza Scopetani:** Writing – review & editing, Formal analysis. **David Chelazzi:** Writing – review & editing, Validation, Data curation. **Tania Martellini:** Writing – review & editing, Supervision. **Alessandra Cincinelli:** Writing – review & editing, Supervision. **Emiliano Carretti:** Writing – review & editing, Supervision, Formal analysis, Data curation. **Miriam Ascolese:** Writing – review & editing, Supervision, Formal analysis, Data curation. **Riccardo Gori:** Writing – review & editing, Supervision, Resources. **Karl Mair:** Resources, Project administration, Funding acquisition. **Werner Tirler:** Resources, Project administration, Funding acquisition. **Massimo Donegà:** Writing – review & editing, Formal analysis, Data curation. **Gianni Andreottola:** Writing – review & editing, Supervision, Project administration, Methodology, Investigation, Funding acquisition, Data curation, Conceptualization.

Acknowledgments

This research did not receive any specific grant from funding agencies in the public, commercial, or not-for-profit sectors. Simone Cavazzoli acknowledges the Italian Ministry of Universities and Research for funding his PhD scholarship (37th Cycle PhD Programmes supported by ESF REACT-EU funds, National Operational Programme on Research and Innovation). The authors would like to thank the Health and Environmental Engineering Laboratories (LISA) at the University of Trento, Eco Center and Eco Research, the Chemistry Laboratories at the University of Florence (DICUS), and those at the Prato Campus of the University of Florence (Fondazione PIN) for their analytical support. We also extend our gratitude to Bopp for providing the steel mesh filters. David Chelazzi, Tania Martellini, Alessandra Cincinelli, and Emiliano Carretti gratefully acknowledge CSGI (Consorzio Interuniversitario per lo Sviluppo dei Sistemi a Grande Interfase - Center for Colloid and Surface Science), Florence (Italy) for financial support. Finally, special thanks to Macrovector for the 'Isometric Composition of Wastewater Treatment' image, which was used in the creation of the graphical abstract.

Appendix A. Supplementary data

Supplementary material associated with this article can be found in the online version at doi:10.1016/j.jes.2025.04.035.

References

Abi Farraj, S., Lapointe, M., Kurusu, R.S., Liu, Z., Barbeau, B., Tufenkji, N., 2024. Targeting nanoplastic and microplastic removal in treated wastewater with a simple indicator. Nature Water 2 (1), 72–83.

Adhikari, S., Kelkar, V., Kumar, R., Halden, R.U., 2022. Methods and challenges in the detection of microplastics and nanoplastics: a mini-review. Polym. Internat. 71 (5), 543–551.

Ali, I., Ding, T., Peng, C., Naz, I., Sun, H., Li, J., et al., 2021. Micro- and nanoplastics in wastewater treatment plants: occurrence, removal, fate, impacts and remediation technologies – a critical review. Chem. Eng. J. 423, 130205.

Anuar Sharuddin, S.D., Abnisa, F., Wan Daud, W.M.A., Aroua, M.K., 2016. A review on pyrolysis of plastic wastes. Energ. Convers. Manage. 115, 308–326.

Bakir, A., Rowland, S.J., Thompson, R.C., 2012. Competitive sorption of persistent organic pollutants onto microplastics in the marine environment. Mar. Pollut. Bull. 64 (12), 2782–2789.

Bassin, J.P., Dezotti, M., 2018. Moving bed biofilm reactor (MBBR). In: Dezotti, M., Lippel, G., Bassin, J.P. (Eds.), Advanced Biological Processes for Wastewater Treatment. Springer International Publishing, pp. 37–74.

Bayo, J., Olmos, S., López-Castellanos, J., Alcolea, A., 2016. Microplastics and microfibers in the sludge of a municipal wastewater treatment plant. Int. J. Sustain. Dev. Plan. 11 (5), 812–821.

Ben-David, E.A., Habibi, M., Haddad, E., Hasanin, M., Angel, D.L., Booth, A.M., et al., 2021. Microplastic distributions in a domestic wastewater treatment plant: removal efficiency, seasonal variation and influence of sampling technique. Sci. Total Environ. 752, 141837.

Blair, R.M., Waldron, S., Phoenix, V., Gauchotte-Lindsay, C., 2017. Micro- and nanoplastic pollution of freshwater and wastewater treatment systems. Springer Sci. Rev. 5 (1–2), 19–30.

Brandt, H.-D., Nentwig, W., Rooney, N., LaFlair, R.T., Wolf, U.U., Duffy, J., et al., 2011. Rubber, 5. Solution rubbers. In: Ullmann's Encyclopedia of Industrial Chemistry. John Wiley & Sons, Ltd., Chichester, UK.

Cavazzoli, S., Ferrentino, R., Scopetani, C., Monperrus, M., Andreottola, G., 2023. Analysis of micro- and nanoplastics in wastewater treatment plants: key steps and environmental risk considerations. Environ. Monit. Assess. 195 (12), 1483.

Cincinelli, A., Scopetani, C., Chelazzi, D., Lombardini, E., Martellini, T., Katsoyiannis, A., et al., 2017. Microplastic in the surface waters of the Ross Sea (Antarctica): occurrence, distribution and characterization by FTIR. Chemosphere 175, 391–400.

Claessens, M., Cauwenberghe, L.V., Vandegehuchte, M.B., Janssen, C.R., 2013. New techniques for the detection of microplastics in sediments and field collected organisms. Mar. Pollut. Bull. 70 (1–2), 227–233.

Corradini, F., Meza, P., Eguiluz, R., Casado, F., Huerta-Lwanga, E., Geissen, V., 2019. Evidence of microplastic accumulation in agricultural soils from sewage sludge disposal. Sci. Total Environ. 671, 411–420.

Debroy, A., George, N., Mukherjee, G., 2022. Role of biofilms in the degradation of microplastics in aquatic environments. J. Chem. Technol. Biotechnol. 97 (12), 3271–3282.

Dehaut, A., Cassone, A.L., Frère, L., Hermabessiere, L., Himber, C., Rinnert, E., et al., 2016. Microplastics in seafood: benchmark protocol for their extraction and characterization. Environ. Pollut. 215, 223–233.

Dong, M., She, Z., Xiong, X., Ouyang, G., Luo, Z., 2022. Automated analysis of microplastics based on vibrational spectroscopy: are we measuring the same metrics? Anal. Bioanal. Chem. 414 (11), 3359–3372.

Dris, R., Gasperi, J., Rocher, V., Saad, M., Renault, N., Tassin, B., et al., 2015. Microplastic contamination in an urban area: a case study in Greater Paris. Environ. Chem. 12 (5), 592..

Duemichen, E., Eisentraut, P., Celina, M., Braun, U., 2019. Automated thermal extraction-desorption gas chromatography mass spectrometry: a multifunctional tool for comprehensive characterization of polymers and their degradation products. J. Chromatogr. A 1592, 133–142.

Endo, S., Takizawa, R., Okuda, K., Takada, H., Chiba, K., Kanehiro, H., et al., 2005. Concentration of polychlorinated biphenyls (PCBs) in beached resin pellets: variability among individual particles and regional differences. Mar. Pollut. Bull. 50 (10), 1103–1114.

Enfrin, M., Dumée, L.F., Lee, J., 2019. Nano/microplastics in water and wastewater treatment processes – origin, impact and potential solutions. Water Res. 161, 621–638.

European Commission, 2023. Commission regulation (EU) amending REACH Regulation as regards synthetic polymer microparticles. Eur. Comm., Brussels, Belgium. Available at: https://eur-lex.europa.eu/eli/reg/2023/2055/oj/eng. Accessed August 30, 2025.

Fischer, M., Scholz-Böttcher, B.M., 2017. Simultaneous trace identification and quantification of common types of microplastics in environmental samples by pyrolysis-gas chromatography-mass spectrometry. Environ. Sci. Technol. 51 (9), 5052–5060.

Galafassi, S., Sabatino, R., Sathicq, M.B., Eckert, E.M., Fontaneto, D., Dalla Fontana, G., et al., 2021. Contribution of microplastic particles to the spread of resistances and pathogenic bacteria in treated wastewaters. Water Res. 201, 117368.

Geyer, R., Jambeck, J.R., Law, K.L., 2017. Production, use, and fate of all plastics ever made. Sci. Adv. 3, e1700782.

Giarrizzo, T., Andrade, M.C., Schmid, K., Winemiller, K.O., Ferreira, M., Pegado, T., et al., 2019. Amazonia: the new frontier for plastic pollution. Front. Ecol. Environ. 17 (6), 309–310.

Hatinoğlu, M.D., Sanin, F.D., 2021. Sewage sludge as a source of microplastics in the environment: a review of occurrence and fate during sludge treatment. J. Environ. Manage. 295, 113028.

Hendrickson, E., Minor, E.C., Schreiner, K., 2018. Microplastic abundance and composition in western lake superior as determined via microscopy, pyr-GC/MS, and FTIR. Environ. Sci. Technol. 52 (4), 1787–1796.

Henshaw, J.M., Wood, V., Hall, A.C., 1999. Failure of automobile seat belts caused by polymer degradation. Eng. Fail. Anal. 6 (1), 13–25.

Hermabessiere, L., Himber, C., Boricaud, B., Kazour, M., Amara, R., Cassone, A.L., et al., 2018. Optimization, performance, and application of a pyrolysis-GC/MS method for the identification of microplastics. Anal. Bioanal. Chem. 410 (25), 6663–6676.

Huppertsberg, S., Knepper, T.P., 2018. Instrumental analysis of microplastics—benefits and challenges. Anal. Bioanal. Chem. 410 (25), 6343–6352.

Hurley, R.R., Lusher, A.L., Olsen, M., Nizzetto, L., 2018. Validation of a method for extracting microplastics from complex, organic-rich, environmental matrices. Environ. Sci. Technol. 52 (13), 7409–7417.

Jani, V., Wu, S., Venkiteshwaran, K., 2024. Advancements and regulatory situation in microplastics removal from wastewater and drinking water: a comprehensive review. Microplastics 3 (1), 98–123.

Jia, W., Karapetrova, A., Zhang, M., Xu, L., Li, K., Huang, M., et al., 2022. Automated identification and quantification of invisible microplastics in agricultural soils. Sci. Total Environ. 844, 156853.

Jiang, X., Wang, T., Jiang, M., Xu, M., Yu, Y., Guo, B., et al., 2020. Assessment of plastic stocks and flows in China: 1978-2017. Resour. Conserv. Recycl. 161, 104969.

Kanold, E., Rillig, M., Antunes, P.M., 2021. Microplastics and phagotrophic soil protists: evidence of ingestion: see video as supplementary material. Soil Organ. 93 (2), 133–140.

Kim, S., Sin, A., Nam, H., Park, Y., Lee, H., Han, C., 2022. Advanced oxidation processes for microplastics degradation: a recent trend. Chem. Eng. J. Adv. 9, 100213.

Kirstein, I.V., Kirmizi, S., Wichels, A., Garin-Fernandez, A., Erler, R., Löder, M., et al., 2016. Dangerous hitchhikers? Evidence for potentially pathogenic *Vibrio* spp. on microplastic particles. Mar. Environ. Res. 120, 1–8.

Lares, M., Ncibi, M.C., Sillanpää, M., Sillanpää, M., 2018. Occurrence, identification and removal of microplastic particles and fibers in conventional activated sludge process and advanced MBR technology. Water Res. 133, 236–246.

Laskar, N., Kumar, U., 2019. Plastics and microplastics: a threat to environment. Environ. Technol. Innov. 14, 100352.

Li, J., Zhang, K., Zhang, H., 2018. Adsorption of antibiotics on microplastics. Environ. Pollut. 237, 460–467.

Markley, L.A.T., Driscoll, C.T., Hartnett, B., Mark, N., Mateos Cárdenas, A., Hapich, H., 2024. Guide for the visual identification and classification of plastic particles doi:10.13140/RG.2.2.27505.45927.

Masura, J., Baker, J., Foster, G., Arthur, C., 2015. Laboratory Methods for the analysis of microplastics in the Marine environment: recommendations for quantifying synthetic particles in waters and sediments. NOAA Marine Debris Program.

Mintenig, S.M., Int-Veen, I., Löder, M.G.J., Primpke, S., Gerdts, G., 2017. Identification of microplastic in effluents of waste water treatment plants using focal plane array-based micro-fourier-transform infrared imaging. Water Res. 108, 365–372.

Nizzetto, L., Futter, M., Langaas, S., 2016. Are agricultural soils dumps for microplastics of urban origin? Environ. Sci. Technol. 50 (20), 10777–10779.

Ogawa, T., Yamasaki, S., Honda, M., Terao, Y., Kawabata, S., Maeda, Y., 2012. Long-term survival of salivary streptococci on dental devices made of ethylene vinyl acetate. Int. J. Oral Sci. 4 (1), 14–18.

Pagliaccia, B., Ascolese, M., Vannini, E., Carretti, E., Lubello, C., Gori, R., 2025. Methodologic insights aimed to set-up an innovative Laser Direct InfraRed (LDIR)-based method for the detection and characterization of microplastics in wastewaters. Sci. Total Environ. 967, 178817.

Pal, D., Prabhakar, R., Barua, V.B., Zekker, I., Burlakovs, J., Krauklis, A., et al., 2024. Microplastics in aquatic systems: a comprehensive review of its distribution, environmental interactions, and health risks. Environ. Sci. Pollut. Res. 32 (1), 56–88.

Palacios-Mateo, C., van der Meer, Y., Seide, G., 2021. Analysis of the polyester clothing value chain to identify key intervention points for sustainability. Environ. Sci. Eur. 33 (1), 2.

Paul, M.B., Stock, V., Cara-Carmona, J., Lisicki, E., Shopova, S., Fessard, V., et al., 2020. Micro- and nanoplastics-current state of knowledge with the focus on oral uptake and toxicity. Nanoscale Adv. 2 (10), 4350–4367.

Penzel, E., 2000. Polyacrylates. In: Wiley-VCH (Ed.), Ullmann's Encyclopedia of Industrial Chemistry, (1st Ed.). Wiley, New Jersey.

Peters, E.N., 2002. Plastics: thermoplastics, thermosets, and elastomers. In: Handbook of Materials Selection. John Wiley & Sons, Ltd., pp. 335–355.

Plastics Europe, 2024. The circular economy for plastics – a European analysis. Plastics Europe, Brussels, Belgium. Available at: https://plasticseurope.org/knowledge-hub/the-circular-economy-for-plastics-a-european-analysis-2024/. Accessed August 30, 2025.

Pittura, L., Foglia, A., Akyol, Ç., Cipolletta, G., Benedetti, M., Regoli, F., et al., 2021. Microplastics in real wastewater treatment schemes: comparative assessment and relevant inhibition effects on anaerobic processes. Chemosphere 262, 128415.

Primpke, S., Christiansen, S.H., Cowger, W., Frond, H.D., Deshpande, A., Fischer, M., et al., 2020. Critical assessment of analytical methods for the harmonized and cost-efficient analysis of microplastics. Appl. Spectrosc. 74 (9), 1012–1047.

Primpke, S., Wirth, M., Lorenz, C., Gerdts, G., 2018. Reference database design for the automated analysis of microplastic samples based on fourier transform infrared (FTIR) spectroscopy. Anal. Bioanal. Chem. 410 (21), 5131–5141.

Queiroz, A.F.dos S., da Conceição, A.S., Chelazzi, D., Rollnic, M., Cincinelli, A., et al., 2022. First assessment of microplastic and artificial microfiber contamination in surface waters of the Amazon Continental Shelf. Sci. Total Environ. 839, 156259.

Rochman, C.M., Hoh, E., Hentschel, B.T., Kaye, S., 2013. Long-term field measurement of sorption of organic contaminants to five types of plastic pellets: implications for plastic marine debris. Environ. Sci. Technol. 47 (3), 1646–1654.

Roscher, L., Halbach, M., Nguyen, M.T., Hebeler, M., Luschtinetz, F., Scholz-Böttcher, B.M., et al., 2022. Microplastics in two German wastewater treatment plants: year-long effluent analysis with FTIR and Py-GC/MS. Sci. Total Environ. 817, 152928.

Rout, P.R., Mohanty, A., Aastha, Sharma, A., Miglani, M., Liu, D., Varjani, S., 2022. Micro- and nanoplastics removal mechanisms in wastewater treatment plants: a review. J. Hazard. Mater. Adv. 6, 100070.

Salmi, P., Ryymin, K., Karjalainen, A.K., Mikola, A., Uurasjärvi, E., Talvitie, J., 2021. Particle balance and return loops for microplastics in a tertiary-level wastewater treatment plant. Water Sci. Technol. 84 (1), 89–100.

Sarti, C., Cincinelli, A., Bresciani, R., Rizzo, A., Chelazzi, D., Masi, F., 2024. Microplastic removal and risk assessment framework in a constructed wetland for the treatment of combined sewer overflows. Sci. Total Environ. 952, 175864.

Scopetani, C., Chelazzi, D., Martellini, T., Pellinen, J., Ugolini, A., Sarti, C., et al., 2021. Occurrence and characterization of microplastic and mesoplastic pollution in the Migliarino San Rossore, Massaciuccoli Nature Park (Italy). Mar. Pollut. Bull. 171, 112712.

Simon, M., van Alst, N., Vollertsen, J., 2018. Quantification of microplastic mass and removal rates at wastewater treatment plants applying Focal Plane array (FPA)-based fourier Transform infrared (FT-IR) imaging. Water Res. 142, 1–9.

Song, Y.K., Hong, S.H., Jang, M., Han, G.M., Rani, M., Lee, J., et al., 2015. A comparison of microscopic and spectroscopic identification methods for analysis of microplastics in environmental samples. Mar. Pollut. Bull. 93 (1–2), 202–209.

Stickler, M., Rhein, T., 2000. Polymethacrylates. Ullmann's Encyclopedia of Industrial Chemistry. Wiley-VCH, Weinheim, Germany.

Stroski, K.M., 2019. Wastewater sources of priority contaminants in four Canadian Arctic Communities. Master Thesis. University of Manitoba, Winnipeg, MB, Canada.

Sun, J., Dai, X., Wang, Q., van Loosdrecht, M.C.M., Ni, B.J., 2019. Microplastics in wastewater treatment plants: detection, occurrence and removal. Water Res. 152, 21–37.

Tagg, A.S., Harrison, J.P., Ju-Nam, Y., Sapp, M., Bradley, E.L., Sinclair, C.J., et al., 2017. Fenton's reagent for the rapid and efficient isolation of microplastics from wastewater. Chem. Commun. 53 (2), 372–375.

Talvitie, J., Mikola, A., Koistinen, A., Setälä, O., 2017a. Solutions to microplastic pollution – removal of microplastics from wastewater effluent with advanced wastewater treatment technologies. Water Res. 123, 401–407.

Talvitie, J., Mikola, A., Koistinen, A., Setälä, O., 2017b. Solutions to microplastic pollution – removal of microplastics from wastewater effluent with advanced wastewater treatment technologies. Water Res. 123, 401–407.

Thompson, R.C., Olson, Y., Mitchell, R.P., Davis, A., Rowland, S.J., John, A.W.G., et al., 2004. Lost at sea: where is all the plastic? Science 304 (5672), 838.

van den Berg, P., Huerta-Lwanga, E., Corradini, F., Geissen, V., 2020. Sewage sludge application as a vehicle for microplastics in eastern Spanish agricultural soils. Environ. Pollut. 261, 114198.

Viršek, M.K., Lovšin, M.N., Koren, Š., Kržan, A., Peterlin, M., 2017. Microplastics as a vector for the transport of the bacterial fish pathogen species *Aeromonas salmonicida*. Mar. Pollut. Bull. 125 (1–2), 301–309.

Ziajahromi, S., Leusch, F.D.L., 2022. Systematic assessment of data quality and quality assurance/quality control (QA/QC) of current research on microplastics in biosolids and agricultural soils. Environ. Pollut. 294, 118629.